Phosphorus Species, Distribution and Bio-availability in Sewage Sludge and Aerobic Granular Sludge

June 2015

Wenli HUANG

Phosphorus Species, Distribution and Bio-availability in Sewage Sludge and Aerobic Granular Sludge

A Dissertation Submitted to

the Graduate School of Life and Environmental Sciences,

the University of Tsukuba

in Partial Fulfillment of the Requirements

for the Degree of Doctor of Environmental Studies

(Doctoral Program in Sustainable Environmental Studies)

Wenli HUANG

Abstract

Phosphorous (P) is an essential and limiting element for living organisms and human beings, especially for the growth of plants. However, phosphate rock, raw material used for P fertilizers, is a non-renewable resource. Thus P resource protection and P recovery is prerequisite for a sustainable agriculture and society on a global scale. On the other hand, sewage sludge generated from wastewater treatment is regarded as a potential P reservoir due to its high production amount and high P content. Moreover, aerobic granular sludge (AGS) is a promising technology for wastewater treatment and the generated AGS contains a high level of P. As not all the forms of P exhibit similar mobility and bio-availability in the sludge, detailed information about P fraction is necessary for both activated sludge and AGS, especially when land application of sludge is taken into consideration. According to the Standards, Measurements and Testing (SMT), total P (TP) in sludge can be fractionated into inorganic P (IP), organic P (OP), non-apatite inorganic P (NAIP) and apatite P (AP). OP and NAIP are considered as potentially mobile and bio-available P.

In addition, identification of P species in sludge is helpful to understand the characteristics and function of P in sludge and thus the mechanisms of P removal through biotechnology. Recent research indicates that phosphorus-31 nuclear magnetic resonance spectroscopy (^{31}P NMR) can be used for analyzing IP (orthophosphate(ortho-P), pyrophosphate(pyro-P) and polyphosphate(poly-P)) and OP species (monoester phosphate(monoester-P), diester phosphate(dister-P) and phosphonates) in sediments, soil and activated sludge since it is able to distinguish multiple P compounds among complex substances.

Therefore, this study aims to fractionate P forms in primary sludge, secondary sludge, digested sludge, nitrifying AGS and enhanced biological P removal (EBPR)-

AGS and evaluate their bio-availability. The IP and OP species in those sludges were also analyzed and discussed. Major results are summarized as follows:

(1) IP was the primary P fraction in the secondary sludge and digested sludge, while OP was the dominant P composition in primary sludge. About 87.7%, 94.8% and 76.2% of TP in primary sludge, secondary sludge and digested sludge, respectively, possessed high potential mobility and bio-availability. Monoester-P and ortho-P were the major P species in primary sludge and digested sludge, respectively, and poly-P was the mainly P species in secondary sludge.

(2) IP was the primary P fraction in nitrifying AGS, in which NAIP amounted to 61.9-70.2%. About 80.9% of TP in nitrifying AGS possessed high potential mobility and bio-availability. Hydroxyapatite [$Ca_5(PO_4)_3(OH)$] and iron phosphate [$Fe_7(PO_4)_6$] patterns were the main IP species in the nitrifying AGS. Monoester-P was the dominant P in OP, and less amount of poly-P was detected in the granules, probably attributable to the inhibition of free ammonia on the activity of phosphorus accumulating organisms (PAOs).

(3) 92.4 - 96.4% of TP in the mature EBPR-AGS exhibited high mobility and bio-availability. The microbial cells, extracellular polymeric substances (EPS) and mineral precipitates respectively contributed 73.7%, 17.6% and 5.2 - 6.4% to the TP of EBPR-AGS. Poly-P occupying 59.2 - 64.1% of TP was the major P species in EBPR-AGS, cells and EPS. Monoester-P and diester-P were identified as the OP species in the AGS and cells. Furthermore, hydroxyapatite [$Ca_5(PO_4)_3OH$] and calcium phosphate [$Ca_2(PO_4)_3$] were the dominant P minerals accumulated in the core of the granules. Cells along with poly-P were mainly in the outer layer of EBPR-AGS while EPS were distributed in the whole granules. Based on the above results, the distribution of IP and OP species in EBPR-AGS has been conceived.

This work would not only be useful for P utilization and recovery from sewage sludge and AGS but also provide insight into the characteristics of P in those sludge, which will help to develop applicable technologies for P removal and recovery through wastewater treatment.

Key words: Sewage sludge; aerobic granular sludge (AGS); phosphorus recovery; phosphorus removal; phosphorus species.

Contents

Abbreviations

AGS: Aerobic granular sludge

AP: Apatite phosphorus

CLSM: Confocal laser scanning microscope

COD: Chemical oxygen demand

DAPI: 4, 6-diamidino-2-phenylindole

Diester-P: Diester phosphate

EBPR: Enhanced biological phosphorus removal

EDX: Energy dispersive X-ray

EPS: Extracellular polymeric substances

IP: Inorganic phosphorus

MLSS: Mixed liquor suspended solids

Monoester-P: Monoester phosphate

NAIP: Non-apatite inorganic phosphorus

^{31}P NMR   31 phosphorus nuclear magnetic resonance spectroscopy

OP: Organic phosphorus

Ortho-P: Orthophosphate

P: Phosphorus

PAOs: Phosphate accumulating organisms

PCA :   Cold perchloric acid

PN: Protein

Poly-P: Polyphosphate

PS: Polysaccharides

Pyro-P: Pyrophosphate

SBRs: Sequencing batch reactors

SEM: Scanning electron microscope

SI: Saturation index

SMT: Standards, Measurements and Testing

SRT: Sludge retention time

SVI: Sludge volume index

TP: Total phosphorus

T(V)S: Total (volatile) solids

UASB: Upflow anaerobic sludge blanket

XRD: X-Ray Diffractomer

WWTP: Wastewater treatment plant

Chapter 1 Introduction

1.1. P resource

P, accounting for around 2 - 4% of the dry weight of most cells, is one of the essential mineral elements for all living organisms, especially for the growth of crops (Karl, 2000). The extensive application of P fertilizers is one of the main reasons that the current crop production has been able to meet the food demand and security associated with an ever-expanding world population. Prior to large-scale mining of phosphate rock for fertiliser production, P was applied to agricultural soils by recycling animal manure, crushed animal bones, human and bird excreta, city waste and ash (Van Vuuren et al., 2010). After the industrial revolution this was replaced by phosphate rock. It is estimated that approximately 60% of the P applied to cropland comes from phosphate rock (Cooper et al., 2011). It is also estimated that around 90% of the P derived from phosphate rock is used in agriculture as fertiliser (Christen, 2007).

On the other hand, phosphate rock, a non-renewable resource, is a naturally occurring geologic material that contains a relatively high concentration of P. The world phosphate rock reserves is around 670 billion tons in 2013 and eight countries or areas including United States, Algeria, China, Jordan, Morocco and Western Sahara, Russia, South Africa and Syria control 93.9% of global reserves; specifically, Morocco and Western Sahara have about 74.6% of total reserves (USGS, 2014). The phosphate rock reserves will be depleted in approximately 300 years in terms of the P production of 2.24 billion tons in 2013. Furthermore, the fertilizer industry recognises that the quality of remaining reserves is decreasing and the cost of extraction,

processing and shipping is increasing (Cordell et al., 2009). Therefore, P resource protection and P recovery is prerequisite for a sustainable agriculture and society on a global scale, especially for the countries that lack of P resources, such as Japan.

1.2. Sludge production and disposal in conventional wastewater treatment plants

Sewage sludge, a by-product of biological wastewater treatment process, is regards as a potential P reservoir due to its high production and P content (Xu et al., 2012). In recent years, the generation of sewage sludge has increased dramatically all over the world because of the elevating rate of wastewater treatment, especially in developing countries. For EU, in 2005, the sludge generation was 2.17×10^6 tons/year (dry solids) in Germany, 1.77×10^6 tons/year (dry solids) in United Kingdom, and 1.12×10^6 tons/year (dry solids) in Spain (Kelessidis and Stasinakis, 2012). In China, the sludge production was amount to 9.0×10^6 tons/year (dry solids) in 2005 and about 3.0×10^7 tons/year (dry solids) in the coming years (He et al., 2007). In Japan, it was estimated that over 2×10^6 tons/year (dry solids) was generated in 2007 and the sludge production steadily increased every year (IWA, 2015).

The huge amount of sludge produced every year already brought about disposal problem to the environment worldwide. Traditionally, there are 4 main methods including land filling, incineration, land application and comprehensive utilization for sludge disposal (Pavšič et al., 2014; Wang, 1997; Kelessidis and Stasinakis, 2012). Among these methods, land application of sewage sludge is now very attractive, because it not only solves the sludge disposal problem but also is of benefit to crop production (Singh and Agrawal, 2008). In EU-15, land application of sludge now is

the predominant choice for sludge management (53% of total amount) (Kelessidis and Stasinakis, 2012). In China, about 45% and 3.5% of sludge is applied to agriculture and gardening, respectively. In Japan, the percentage of treated sewage sludge for farmland and green areas has been stable at around 14% for many years (IWA, 2015). Sewage sludge can provide many easily available nutrient sources like N, K and organic matters, especially P element. Generally, P content in sewage sludge accounts for about 1-5% of total solid. Thus, sewage sludge is considered as an important P fertilizer and resource when land application is taken into consideration, which can partially replace the chemical P fertilizer and to improve the structure and property of soil, thus avoiding soil impoverishment because of the frequent use of chemical fertilizers.

1.3. Granulation technology

1.3.1. Anaerobic granular sludge

Anaerobic granular sludge was first reported by Young and McCarty (1969) in an anaerobic filter system. While, UASB reactor, which developed in the late 1970s, is considered as one of the most effective anaerobic reactors for anaerobic granules cultivation. Anaerobic granules possess some advantages like low operation cost, high biomass, less sensitive to fluctuations of the environmental parameters and low sludge production compared to conventional activated sludge processes (Lim and Kim, 2014). Anaerobic granular biomass is reported to be 20 - 40 g/L in UASB reactor, higher than conventional activated sludge systems (Mahmoud et al., 2004). The high anaerobic granular biomass in a UASB reactor can effectively convert 90-95% organic substance to biogas (Lim and Kim, 2014). The produced methane gas can be utilized

for an energy source of power generation. The output of anaerobic granular sludge in a UASB is much smaller than that in a conventional activated sludge process as only approximately 5%-10% of organic matter transferred to sludge (Lim and Kim, 2014). On the other hand, anaerobic granular sludge can offer various engineering advantages over flocculent anaerobic sludge, such as high solid retention time due to its excellent settling property, providing maximum microorganisms to space ratio, and application of higher loading rates as compared to flocculent sludge. Therefore, thousands of high-rate anaerobic granular sludge reactors have been operated all over the world, especially Europe, South America, South and South East Asia (Franklin, 2001). Most of these reactors are used to treat brewery, beverage, distillery, fermentation, food leachate, pulp, dairy, textile, and paper wastewaters. While the main disadvantages of anaerobic granular sludge are long start-up period and low nutrient removal, especially for ammonia and P, and the effluent from anaerobic digestion needs to be treated before discharged into the environment.

1.3.2. Aerobic granular sludge

Twenty years ago AGS was first reported by Mishima and Nakamura (1991) in a continuous upflow aerobic sludge blanket bioreactor. Compared to conventional activated sludge processes, AGS is a promising biotechnology which possesses many incomparable advantages: (1) the settling time of AGS is less than 30 min, which is much shorter than that of activated sludge. The excellent settleability of AGS significantly decreased volume requirement for the secondary settling tank. (2) AGS has high capacity to withstand toxicity and loading rate because of the compact microstructure of granules with diameter of 0.3-5 mm leading to a concentration gradient which can protect bacteria in the granules (Jemaat et al., 2014). Currently there are more than 20 wastewater treatment plants in operation or under construction

4

using AGS technology (Nereda, 2015). Therefore, in the near future, it is expected that the AGS technology can be applied in the world as one of major processing units in wastewater treatment plants. Liu et al. (2005) calculated the theoretical growth yield of aerobic granules as 0.2 g VSS/g COD removed. Although this value related to sludge production reduced around 33% compared to the conventional activated sludge characterized by a sludge growth yield of around 0.3 g VSS/g COD removed (Heijnen and van Dijken, 1992), lots of AGS will be produced with its gradually application in WWTP.

On the other hand, the dense spherical structure of AGS also can promote P accumulation in granules. In the EBPR processes, as PAOs can be present inside the granules, anaerobic phosphate release can encourage P precipitation within the core of the microorganisms, where subsequent solubilization of the crystals would be more difficult than in the bulk (Angela et al., 2011). In addition, previous studies also reported that P-rich AGS could be achieved during simultaneous nitrification and denitrification processes (Lin et al., 2012; Li et al., 2014). Therefore, high content of P was also accumulated in the AGS, which could be more prospectively used for P fertilizer after being properly treated.

1.4. P fraction and species

As well known that not all the forms of P exhibit similar mobility and bio-availability in the sludge, detailed information about P fraction is necessary for both activated sludge and AGS, especially when land application of sludge is taken into consideration. Many sequential extraction procedures for the determination of P fractions in soil, sediment and sewage sludge have been developed. The SMT, which was developed within the framework of the SMT Programme of the European

Commission, was considered as a harmonized protocol for P fraction which includes three independent extraction procedures and separate P into TP, IP, OP, NAIP and AP (Ruban et al., 1999; Medeiros et al., 2005). Some researchers declared that IP and NAIP were the dominant P forms in secondary sludge, in which the concentration of NAIP + OP was more than 75% and 85% of TP for sludge samples fed with industrial and domestic wastewaters, respectively (Xie et al., 2011b). This suggests the high potential mobility and bioavailability of P existed in activated sludge, which is much meaningful for land application of secondary sludge. Generally, the sludge could be classified as primary sludge, secondary sludge and digested sludge in the wastewater treatment plant. Up to now, however, little information could be found about P fraction and bio-availability in primary sludge, digested sludge and AGS.

Moreover, identification of P species in sewage sludge and AGS is helpful to understand the characteristics and function of P in sludge and thus the mechanisms of P removal and transformation through biological processes. Recent research indicates that ^{31}P NMR can be used for analyzing inorganic and organic P species (ortho-P, pyro-P, poly-P, monoester-P, diester-P and phosphonates) in sediments, soil and activated sludge since it is able to distinguish multiple P compounds among complex substances (Uhlmann et al., 1990; Ahlgren et al., 2011; Li et al., 2013). Poly-P and ortho-P was the major P in enhanced P removal activated sludge and digested sludge, respectively (Hinedi et al., 1989; Uhlmann et al., 1990). In the waste activated sludge and aerobically digested sludge, more than 50% of the TP was present as monoester-P and diester-P (Hinedi et al., 1989). To date, as for AGS, lab-scale experiments have been conducted on the mineral forms of P, demonstrating that the major IP species in AGS are hydroxyapatite, struvite, or Ca-Mg phosphate and whitlockite [$Ca_3(PO_4)_2$], greatly depending on influent characteristics and operation conditions (Angela et al.,

2011; Lin et al., 2012; Li et al., 2014). Nevertheless, other P species and the distribution of IP (IP, like ortho-P, pyro-P and poly-P) and OP (OP, like monoester-P and diester-P) in AGS which are closely related with P removal and recovery, have not been documented yet.

1.5. Research objectives and thesis structure

As mentioned above, P as a non-renewable resource is a necessary element for all livings. The sludge produced from WWTP is considered as a potential P reservoir and has been partially used for crops production as P fertilizer. Moreover, the AGS is a promising process due to its excellent advantages compared with conventional activated sludge process. However, the P species, fraction and bio-availability have not been comprehensively and systematically analyzed in sewage sludge and AGS. The objectives of this study were to analyze the P species, distribution and bio-availability in these sludges, which would not only be useful for P utilization and recovery from sewage sludge and AGS but also provide insight into the functions and characteristics of P in sludge. This work will help to develop applicable technologies for P removal and recovery through wastewater treatment.

The structure of the thesis is illustrated by the experimental framework shown in Figure 1-1. The contents of this thesis are divided into the following three parts so as to comprehensively analyze and evaluate the P in different kinds of sludge.

In Chapter 2, the study focused on P species and fraction analysis in primary sludge, secondary sludge and digested sludge. According to the P forms, the bio-availability of P was obtained from sewage sludge.

Chapter 3 was to identify the inorganic and organic species of P and its bio-availability in nitrifying AGS. Firstly, nitrifying AGS was cultivated in a lab-scale

SBR with high level of ammonium influent. Secondly, the P forms were fractionated and evaluated its bioavailability in nitrifying AGS during the whole cultivation process. Then, the mineral IP was identified by XRD and EDS. Finally, the inorganic and organic P species in nitrifying AGS was analyzed by using ^{31}P NMR spectroscopy.

Chapter 4 investigated the distribution and bio-availability of IP and OP species in EBPR-AGS. Firstly, the architectures of cells, EPS and P distribution were visualized in the granules. Then, IP and OP species in AGS, cells and EPS were further analyzed by using ^{31}P NMR spectroscopy. Finally, based on the obtained results, P distribution in the granules was conceived to better understand the nature of P in EBPR-AGS.

Objective: P species, distribution and bio-availability in sewage sludge and aerobic granular sludge

Sewage sludge

Aerobic granular sludge

Primary sludge

Secondary sludge

Digested sludge

Nitrifying AGS

EBPR-AGS

IP and OP species analysis

Phosphorus fractionation

IP and OP species analysis

Phosphorus fractionation

Mineral P species analysis

IP and OP distribution

^{31}P NMR

SMT protocol

IP : ortho-P, pyro-P ,poly-P
OP: monoester-P, diester-P, phosphonate

Bio-available P (NAIP+OP) evaluation

IP, OP, non-apatite IP (NAIP), apatite P (AP)

AGS, microbial cell, EPS and mineral precipitate

Figure 1-1 Experimental framework of this study. IP, inorganic P; OP, organic P; EBPR, enhanced biological P removal; EPS, extracellular polymeric substances; AGS, aerobic granular sludge; SMT, Standards, Measurements and Testing; NMR, nuclear magnetic resonance.

Chapter 2 P species and bio-availability analysis in sewage sludge

2.1. Introduction

Agricultural utilization of sewage sludge as P fertilizer has been applied for many years not only due to it is an economically attractive alternative to dispose sludge but also due to sewage sludge contains high concentration of P with high output. Identification of the P fraction and species in the sludge is beneficial for both land application of sewage sludge as P fertilizer and understanding the characteristics and function of P in different sludges. Generally, primary sludge, secondary sludge and digested sludge are the three main sludges produced from WWTP. Previous works reported the bio-availability of P in secondary sludge and the P species in secondary sludge and digested sludge (Xie et al., 2011b; Hinedi et al., 1989). To date, little detailed and comprehensively information could be found about the P fractions and species in primary sludge, secondary and digested sludge. Therefore, the main objective in this study was to investigate the fractionation and species of P in primary sludge, secondary sludge and digested sludge, and to evaluate the mobility and bio-availability of P in various sludges.

2.2. Materials and methods

2.2.1. Sewage sludge sample

Sludge samples were collected from a WWTP treating domestic wastewater in Shimodate, Ibaraki Prefecture, Japan. The process flow diagram of the WWTP is

shown in Figure 2-1.The sludge samples were collected from the primary tank, sedimentation tank and digestion tank, respectively. The collected sludge was kept in a refrigerator at 4 ℃ and analyzed within 2 days.

2.2.2. P fractionation in sludge

In this study, the SMT programme extraction protocol was applied to analyze P fractions in all sludge samples (Figure 2-2), which has been widely used in soil, sediment and sewage sludge samples (Ruban et al., 1999; Medeiros et al., 2005). After sequential extraction based on the SMT method, P in sludge was fractionated into the following 5 categories: (1) TP, (2) OP (3) IP, (4) NAIP, the P fraction associated with oxides and hydroxides of Al, Fe and Mn, and (5) AP, the P fraction associated with Ca. In order to avoid the transformation of P species in sludge during preparation, the samples taken from the reactors were frozen immediately at -80℃, lyophilized at -50℃ for 48 h and stored at -20℃ until analysis. The P concentration in the supernatant collected after extraction was determined with molybdenum blue method.

2.2.3. Extraction of P from sludge.

PCA and NaOH extraction methods have been efficiently used for IP and OP extraction from sludge, soil and sediment samples (Ahlgren et al., 2005; Daumer et al., 2008; Vestergren et al., 2012). In this study, the PCA-NaOH extraction procedure was applied to fractionate and characterize P in the sludge samples according to the schematic diagram shown in Figure 2-3. Before extraction, a certain amount of sludge was washed twice with 100 mM NaCl solution (4℃) with the supernatant being discharged. After extraction, neutralization was conducted immediately to minimize P transformation. 2 ml of the resultant supernatant was taken for TP, IP and OP analysis.

The remaining extracts were freeze-dried at -50℃ for 48 h, and the dried PCA-NaOH extracts were uniformly mixed and them stored at -20℃ till ^{31}P NMR analysis.

2.2.4. Analytical method

T(V)S, COD, NH_4-N, PO_4-P and TP were measured in accordance with the standard methods (APHA,1998). TP in the liquid was determined with molybdenum blue method after digestion by potassium persulfate at 120℃..

To obtain the ^{31}P NMR spectrum, 200 mg of freeze-dried sludge extracts were re-dissolved in 0.8 ml of 1M NaOH and 0.2 ml D_2O followed by 0.2 ml of 100 mM EDTA solution. In order to ensure consistent chemical shifts and optimal spectral resolution during the NMR measurement, EDTA and NaOH solutions were dosed to minimize the interference of divalent/trivalent cations and to adjust the sample pH above 12.0, respectively.

The ^{31}P NMR spectrum was obtained by using a Bruker Avance-600MHz NMR Spectrometer (Bruker, AVANCE-600, USA) at 242.94 MHz. 90℃ of pulse width, 25℃ of regulated temperature, and acquisition time of 0.67 s (with relaxation delay of 2 s) were applied in the experiments. To obtain accurate phosphorus forms, the spectra were collected immediately after preparation and the whole process was completed within 2 h to minimize the transformation of P species. Chemical shifts of signals were determined relatively to an external standard of 85% H_3PO_4 via signal lock. The peaks were assigned to P species according to the reports in literature with peak areas calculated by integration (Ahlgren et al., 2005; Turner et al., 2003; Turner, 2004; Zhang et al., 2013a). In brief, the target P peaks were those in the NMR spectra for ortho-P (5 to 7 ppm), monoester-P (3 to 5 ppm), diester-P (2 to -3 ppm), pyro-P (-4.5 to -6 ppm), poly-P (-4 to -5 and -18 to 21 ppm), and phosphonate (22 to 24 ppm).

2.3. Results and discussion

2.3.1. Variation in solid content of the sludge samples

The TS, TVS and TVS/TS ratio of the sludge are shown in Figure 2-4. The concentration of TS in primary sludge is about 21.9 g/l, which was approximately 2 times of those in secondary and digested sludge. The TVS/TS ratios of primary sludge, secondary sludge and digested sludge were 85.9%, 81.2% and 68.1%, respectively. In anaerobic digestion stage, most biodegradable organic substances can be converted to biogas, leaving most inorganic and recalcitrant materials in the digested sludge. This can be explained the lower TVS/TS ratio of digested sludge than those of primary sludge and secondary sludge.

2.3.2. P fractionation in sludge by SMT protocol

Table 2-1 summarized the P fractions of primary sludge, secondary sludge and digested sludge, respectively. The TP concentration in secondary sludge was about 46.1 mg/g-TS, which was around 4.3 times of that in primary sludge. This result may be brought about by the secondary sludge responsible for P removal from wastewater has accumulated high concentration of P, while the primary sludge directly settled from wastewater is mainly suspended solid contaminants. Compared to secondary sludge, lower concentration of TP in digested sludge was also detected, most probably due to parts of P in the secondary sludge was released to the effluent from digestion tank (Table 2-2). OP content of secondary sludge was about 19.1 mg/g-TS, much higher than those of primary sludge (7.6 mg/g) and digested sludge (5.2 mg/g). While the percentage of OP to TP was 71.7% in primary sludge, which was higher than those

of secondary sludge (41.4%) and digested sludge(16.3%), indicating OP is the dominant P in primary sludge (Figure 2-5). Ahlgren et al (2011) claimed that OP can be released from sediments and utilized by algae. Moreover, OP in soil can be hydrolyzed by phosphatase and then used by the rhizosphere of plants (George et al., 2006). Thus high content of OP in sludge may play an important role in P recycle when land application of sludge as P fertilizer is taken into consideration.

On the other hand, IP was the major P fraction in secondary sludge and digested sludge, in which IP accounted for 58.4% and 77.5% of TP, respectively. Only about 3.1 mg/g IP, about 28.8% of TP was detected in primary sludge (Table 2-1, Figure 2-5). NAIP was the dominant IP in primary sludge, secondary sludge and digested sludge, accounting for 55.8%, 91.6% and 69.3% of IP, respectively. In addition, NAIP was about 16.0%, 53.4% and 59.9% of TP in primary sludge, secondary sludge and digested sludge, respectively. Compared with OP and NAIP, AP content was relatively low, about 13.2% of TP in primary sludge and 5.6% of TP in secondary sludge. However, a high content and percentage of AP was founded in digested sludge (8.2 mg/g and 25.7% of TP), most probably due to the formation of Ca-P precipitates in the digestion tank resulting from the saturation status of co-existing calcium phosphate.

OP and NAIP were considered to be releasable and bio-available P. In this study, the concentration of NAIP+OP were 9.3, 43.7 and 24.3 mg/g-TS, accounting for about 87.7%, 94.8% and 76.2% in primary sludge, secondary sludge and digested sludge, respectively. It was obviously that secondary sludge not only has the highest NAIP+OP content but also has the highest percentage of NAIP+OP among the three sludge samples. Although digested sludge has the lowest percentage of NAIP+OP, its NAIP+OP contents are much higher than those in primary sludge. These results

14

suggest that primary sludge, secondary sludge and digested sludge can be used as P resource materials due to their high potential mobility and bioavailability of P.

2.3.3. Identification of P species in sludge by ^{31}P NMR analysis

Quantification of various P fractions by integrating the peak areas in NMR spectra has been widely used to estimate the relative proportions of P fractions. All NMR-spectra show peaks in the areas for ortho-P, monoester-P, diester-P, pyro-P, poly-P (Figure 2-6). Table 2-3 summarizes the contents of these compounds and their relative proportions (% TP) in primary sludge, secondary sludge and digested sludge extracts identified by ^{31}P NMR. The average TP contents in the PCA + NaOH extracts from primary sludge, secondary sludge and digested sludge were 9.7, 43.4 and 29.8 mg-P/g-TS with average extraction rate of approximately 91.5-94.1% of TP, respectively, indicating the high efficiency of PCA + NaOH procedure for P extraction from sludge samples.

In primary sludge extracts, ortho-P, monoester-P and diester-P are identified as the major P species, accounting for approximately 21.3, 54.6 and 24.1% of TP, respectively. Obviously, the monoester-P and diester-P are the dominant OP species in primary sludge extracts. Generally, monoester-P and diester-P are regarded as potential bio-available P due to that they can be hydrolyzed and utilized by plants and algal in certain conditions. In the secondary sludge, poly-P was the major form of P species, comprising 54.2% of the extractable TP from sludge (Table 2-3). The high content of poly-P in secondary sludge signals the high amount and bioactivity of PAOs in activated sludge in the aeration tank during sampling period. Specifically, pyro-P was only identified in the secondary sludge, around 2.4% of extractable TP. The presence of pyro-P could indicate microbial activity in sludge due to it is directly

related to adenosine triphosphate (ATP) hydrolysis in cells. Ortho-P, a main nutrient for living organisms, was about 89.2% of TP in the digested sludge, which was much higher than those in the primary sludge and the secondary sludge. This result indicate that all poly-P and pyro-P in secondary sludge, most of monoester-P and diester-P in primary sludge and secondary sludge were most probably converted to ortho-P or reused by anaerobic bacteria during digestion process.

2.4. Summary

In this part, the P species and bio-availability in primary sludge, secondary sludge and digested sludge were identified and evaluated. The following results can be obtained:

(1) IP was the primary P fraction in the secondary sludge and digested sludge, in which NAIP amounted to 91.6% and 69.3%, respectively. OP content (about 7.6 mg/g-TS) was the dominant P in the primary sludge. About 87.7%, 94.8% and 76.2% of TP possesses high potential mobility and bio-availability for primary sludge, secondary sludge and digested sludge, respectively.

(2) Two OP fractions (monoester-P and diester-P) and three IP compounds (ortho-P, poly-P and pyro-P) were identified P species in the secondary sludge. Poly-P was the dominant P species in the secondary sludge, comprising approximately 54.3% of TP. Monoester-P and ortho-P, accounting for 54.6% and 89.2% of TP, were the major P species in the primary sludge and digested sludge, respectively.

These results revealed that the proportion and content of P species were different in primary sludge, secondary sludge and digested sludge, and high potential bio-available P were stored in these sludges, which is much meaningful for P removal and recovery from wastewater and sludge in WWTPs.

Table 2-1 Average content of each P fraction in the sludges by using the SMT extraction protocol

Sludge	TP	OP	IP	NAIP	AP	OP+NAIP	Bio-availability
	(mg-P/g-TS)	(mg-P/g-TS)	(mg-P/g-TS)	(mg-P/g-TS)	(mg-P/g-TS)	(mg-P/g-TS)	(%)
Primary sludge	10.6±3.2	7.6±2.4	3.1±1.6	1.7±0.8	1.4±0.6	9.3	87.7
Secondary sludge	46.1±5.6	19.1±3.5	26.9±2.8	24.6±3.1	2.6±1.1	43.7	94.8
Digested sludge	31.9±5.1	5.2±2.9	26.7±3.4	19.1±2.3	8.2±2.7	24.3	76.2

TS, total solids; TP, total P; OP, organic P; IP, inorganic P; NAIP, non-apatite P; AP, apatite P; Bio-availability, the percentage of OP+NAIP to TP.

Table 2-2 Variation of COD, NH_4-N, TP, and PO_4-P in the influent and effluent from the treatment units of the WWTP

Treatment units	COD (mg/l)	NH_4-N (mg/l)	TP (mg/l)	PO_4-P (mg/l)
Influent	205.3	28.3	3.0	2.3
Primary settling tank effluent	248.8	30.2	3.5	3.4
Digestion tank effluent	714.2	636.9	241.4	211.8
Effluent	19.3	1.3	0.2	0.1

COD, chemical oxygen demand; TP, total phosporus.

Table 2-3 Contents of different P fractions extracted by PCA + NaOH method and their relative

proportions (%TP) identified by ^{31}P NMR in the sludge samples

Sample	TP$_{Extract}$	IP			OP	
		Ortho-P	Pyro-P	Poly-P	Monoester-P	Diester-P
	(mg-P/g-TS)	(%)	(%)	(%)	(%)	(%)
Primary sludge	9.7±2.8	21.3±3.1	-	-	54.6±5.7	24.1±4.2
Secondary sludge	43.4±4.7	17.6±6.5	2.4±1.2	54.2±5.7	16.1±4.9	9.7±2.2
Digested sludge	29.8±4.1	89.2±5.8	-	-	6.6±3.3	4.3±3.6
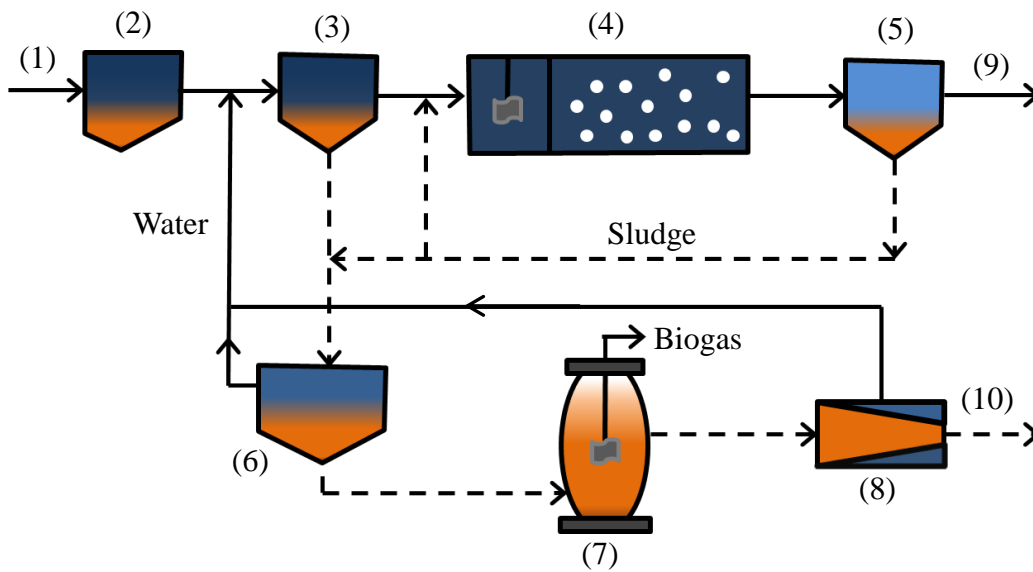
Figure 2-1 Process flow diagram of wastewater treatment plant in Shimodate, Ibaraki Prefecture, Japan. (1) influent, (2) grid, (3) primary settling tank, (4) aeration tank, (5) secondary settling tank, (6) sludge concentration tank, (7) digestion tank, (8) sludge dewatering, (9) effluent, (10) sludge disposal.
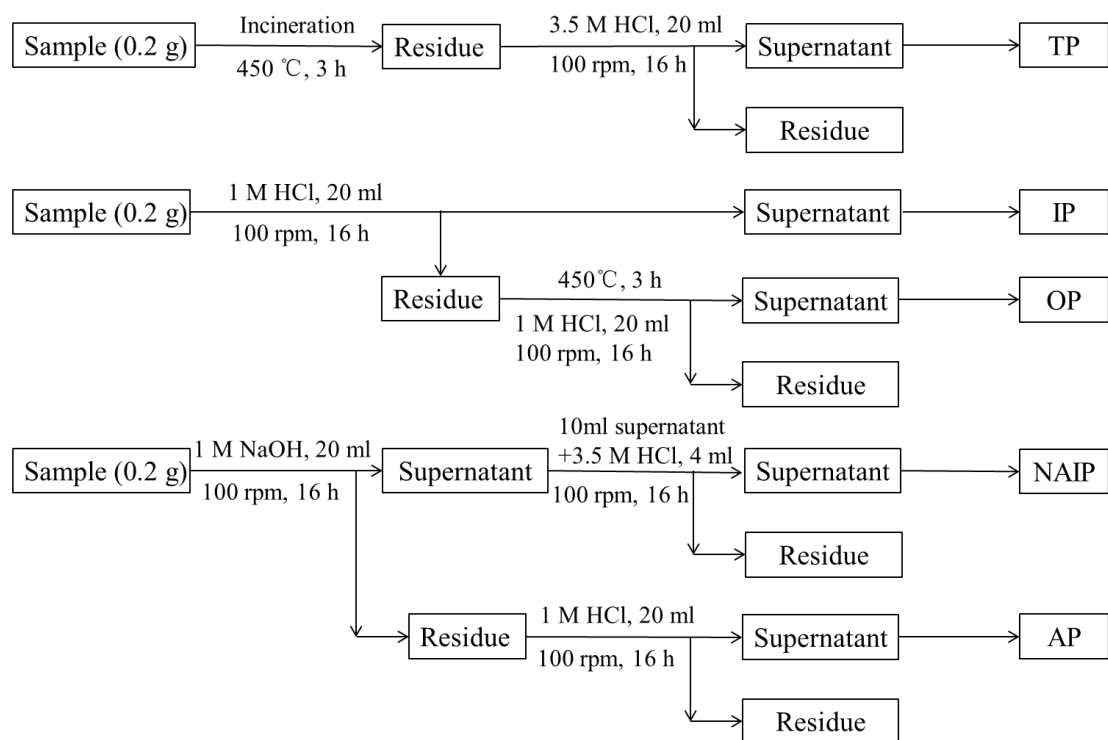
Figure 2-2 The schematic diagram of the SMT protocol (Ruban et al., 1999; Medeiros et al., 2005).
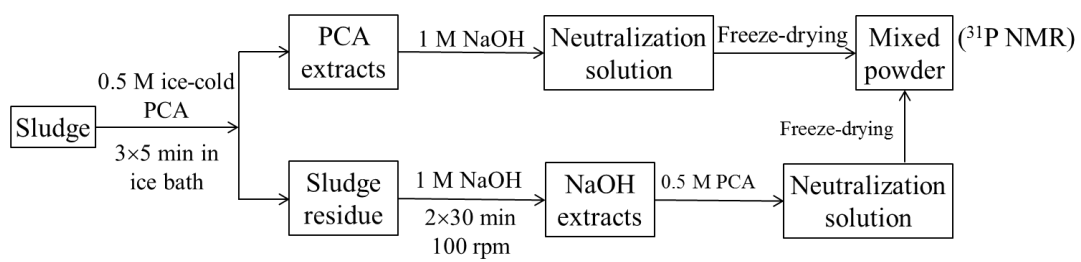
Figure 2-3 Schematic diagrams for the fractionation and characterization of various forms of P in sewage sludge.
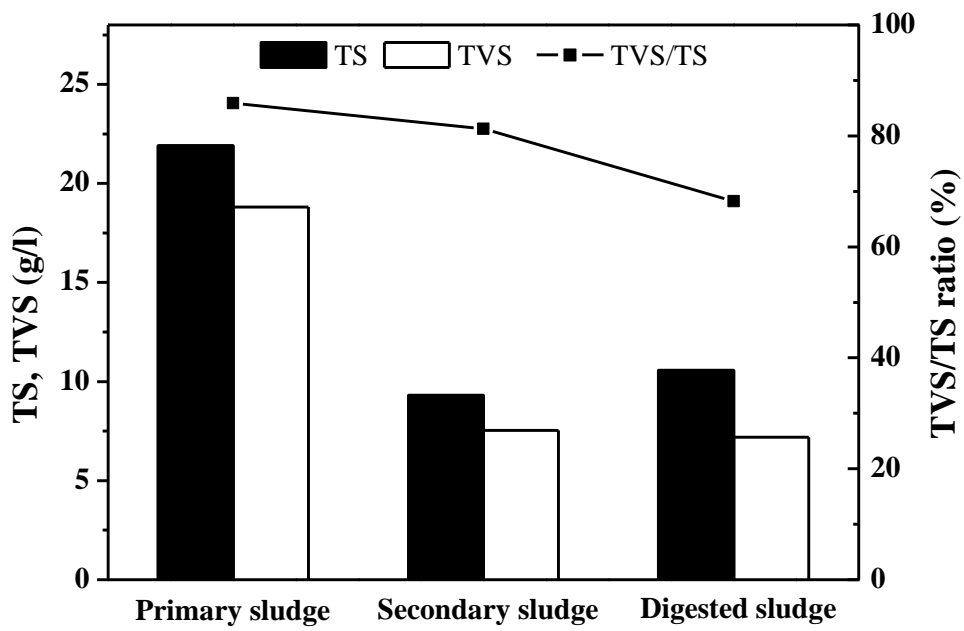
Figure 2-4 Changed in TS, TVS and TVS/TS ratio of the sludge sample.
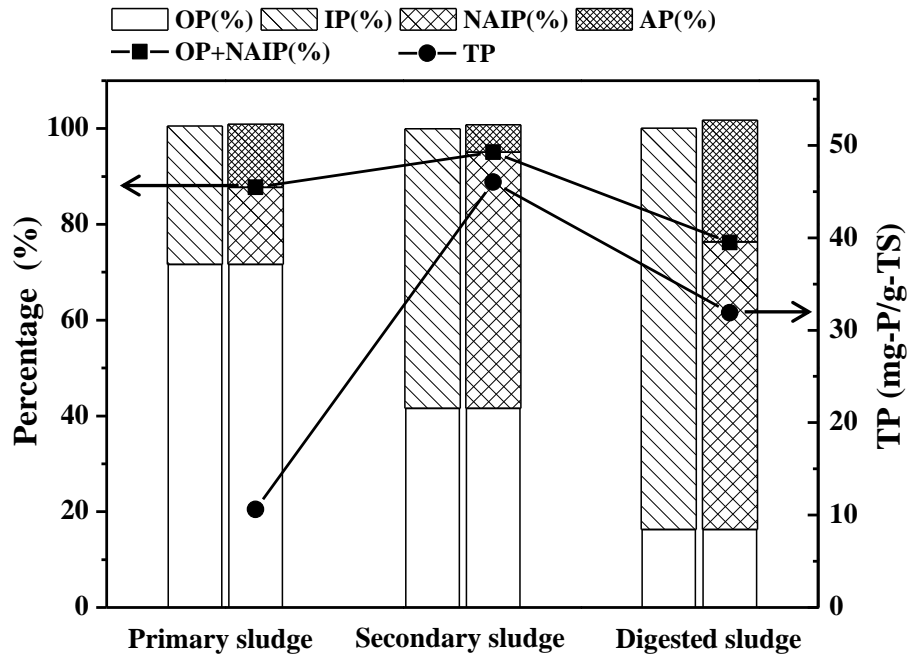
Figure 2-5 TP concentrations and percentage of each P fraction to TP in the sludges by using the SMT extraction protocol. TS, total solids; TP, total phosphorus; OP, organic phosphorus; IP, inorganic phosphorus; NAIP, non-apatite inorganic phosphorus; AP, apatite phosphorus.
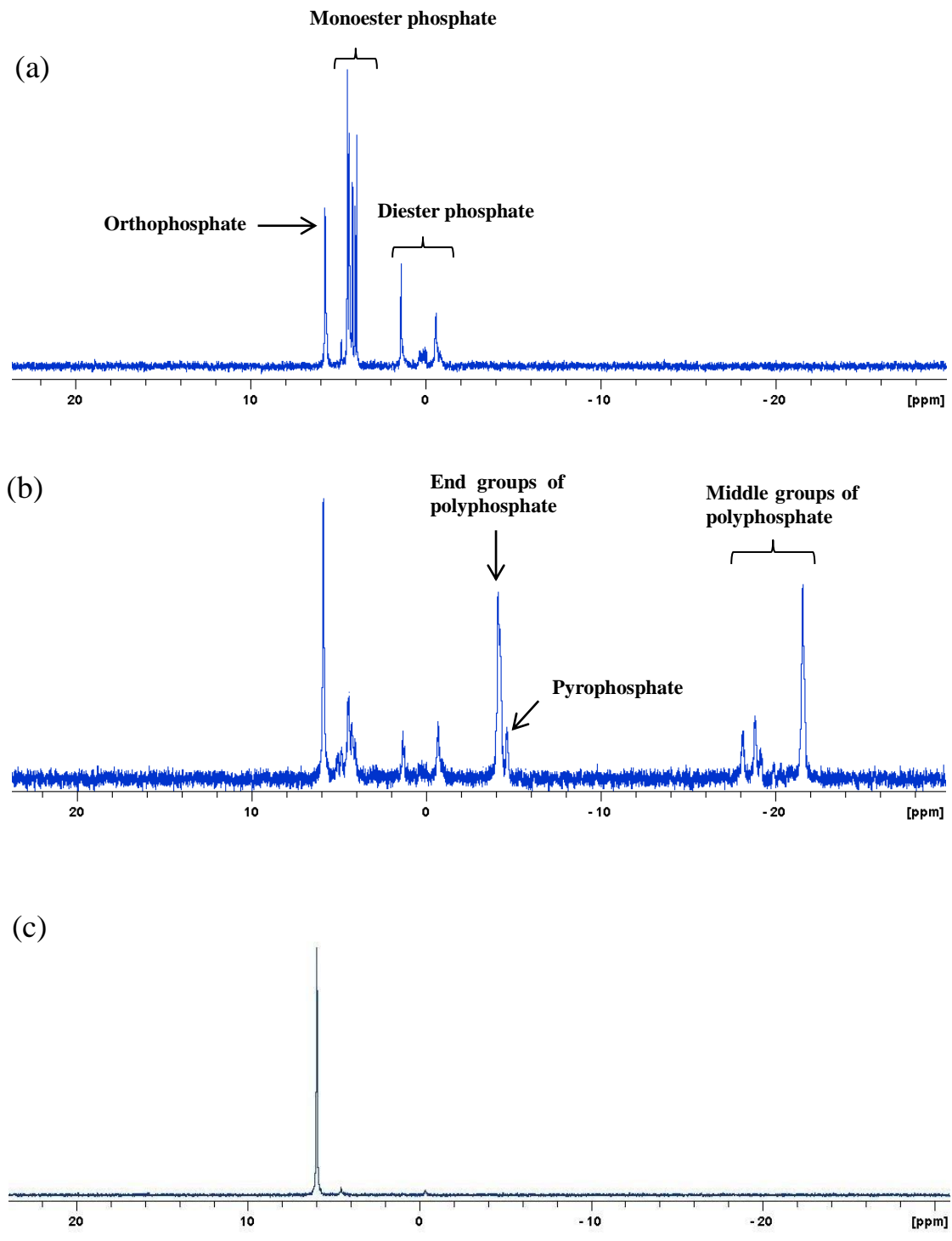
Figure 2-6 Typical ^{31}P NMR spectra of PCA+NaOH extracts from (a) primary sludge,

(b) secondary sludge and (c) digested sludge.

Chapter 3 Identification of inorganic and organic species of P and its bio-availability in nitrifying AGS

3.1. Introduction

Nitrifying AGS is one kind of granules that mainly responsible for removal ammonia from wastewater. Compared with conventional nitrifying activated sludge processes, nitrifying AGS is a promising biotechnology for nitrogen removal from wastewater due to it not only possess advantages like excellent settleability and high biomass but also could accumulate much higher nitrifying bacteria in the granules thus withstand high ammonia loading rate (Qin et al., 2004; Yilmaz et al., 2008; Adav et al., 2008a; Wang et al., 2012). Previous studies reported that P-rich aerobic granules could be achieved during simultaneous nitrification and denitrification processes (Lin et al., 2012; Li et al., 2014), indicating that nitrifying AGS can be used for P fertilizer after being properly treated. Up to now, however, little information can be found in the literature about the IP and OP species and its bio-availability in nitrifying AGS. Therefore, this study aims to reveal the fractionation and distribution of P in nitrifying AGS and to evaluate the mobility and bio-availability of P in granules. In addition, OP and IP species in the granules were also determined and characterized. It is expected that this work would not only be useful for P utilization and recovery from AGS but also provide insight into the characteristics of P in AGS.

3.2. Materials and methods

3.2.1. Experimental set-up and operation

Nitrifying AGS were cultivated in two identical SBRs made of acrylic plastic with height of 60 cm and square cross section of 6 cm×6 cm. Their effective working volume was 1.4 l. Aeration was provided by an air pump (AK-30, KOSHIN, Japan) through air bubble diffusers at the bottom of each reactor with an air flow rate of 2.0 cm/s and the dissolved oxygen (DO) maintained at 7-9 mg/l during aeration. Synthetic wastewater was used in this study, and its composition was as follows: COD 600 mg/l (50% of which was contributed by glucose and sodium acetate, respectively); 10 mg PO_4-P/l (KH_2PO_4); 100 mg NH_4-N/l (NH_4Cl) during the first 60 days' operation and then increased to 200 mg NH_4-N/l till the end of experiment; 10 mg Ca^{2+}/l ($CaCl_2$); 5 mg Mg^{2+}/l ($MgSO_4 \cdot 7H_2O$); 5 mg Fe^{2+}/l ($FeSO_4 \cdot 7H_2O$); and 1ml/l of trace element solution. The trace element solution contained (in mg/l) H_3BO_3 (50), $ZnCl_2$ (50), $CuCl_2$ (30), $MnSO_4 \cdot H_2O$ (50), $(NH_4)_6Mo_7O_{24} \cdot 4H_2O$ (50), $AlCl_3$ (50), $CoCl_2 \cdot 6H_2O$ (50), and $NiCl_2$ (50) (Adav et al., 2008b). The pH in the reactors was adjusted with sodium bicarbonate to be within 7.5-8.0.

Each reactor was inoculated with 0.5 l of seed sludge sampled from a sedimentation tank in the Shimodate Sewage Treatment Plant, Ibaraki Prefecture, Japan. The initial MLSS concentration was 4.6 g/l with SVI_{30} of 81.4 ml/g and MLVSS/MLSS of 0.8 in the two reactors. After aerobic granules appeared, the mixed liquor was withdrawn daily from the reactors in order to keep their SRT around 40 days. The reactors were operated sequentially in a 4-h cycle at room temperature (25 ±2℃): 2 min of influent filling, 28 min of non-aeration period, 186-206 min of aeration, 2-20 min of settling, and 4 min of effluent discharge. The settling time was

gradually decreased from 20 min to 2 min due to the increase in settleability of the sludge. The volumetric exchange ratio was kept at 54%, resulting in a hydraulic retention time of 7.4 h.

3.2.2. Chemical and physical analysis

ML(V)SS, SVI_{30}, COD, ammonia nitrogen (NH_4-N), nitrite nitrogen (NO_2-N), nitrate nitrogen (NO_3-N), and PO_4-P were measured in accordance with standard methods (APHA,1998). DO concentration in the bulk liquid was measured with a DO meter (HQ40d, HACH, USA). pH was determined by using a pH meter (Mettler Toledo FE20, Switzerland). Metal ions in sludge samples were quantified after the sludge samples being digested and filtered through 0.22 μm cellulose nitrate membrane filters (Nalgene). 0.1 g of dried sludge was digested in a mixture of 3 ml hydrochloric acid (37%, Wako), 1 ml nitric acid (70%, Wako), and 1 ml perchloric acid (60%, Wako) on an electric heating plate for 10 min. The concentration of each metal was measured by inductively coupled plasma mass spectrometry (ICP-MS, ELAN DRC-e, Perkin Elmer, USA).

The mean granular size was measured by a stereo microscope (STZ-40TBa, SHIMADZU, Japan) with a program Motic Images Plus 2.3S (Version 2.3.0). Morphology characteristics of the granules were observed using a SEM (JSM6330F, Japan). XRD analysis was performed using a Multiflex diffractometer (Rigaku, Japan) with a cobalt tube scattering from 5 to 75° in 2θ. The samples used for XRD analysis were previously dried and calcined in an oven at 500℃ for 2 h in order to remove the organic fraction.

Average values were taken for all the determinations and used for results and discussion.

3.2.3. P fractionation in AGS

In this study, the SMT programme extraction protocol was applied to analyze phosphorus fractions in the nitrifying AGS, which has been shown in Figure 2-2.

3.2.4. P extraction from AGS and analysis by ^{31}P NMR

Nitrifying AGS taken from each reactor was also frozen immediately at -80℃, lyophilized, and ground to fine powders. Then P was extracted from 2 g of the prepared sludge powder with 40 ml of a solution consisting of 0.25 M NaOH and 0.05 M Na_2EDTA (Turner et al., 2003). The mixture was shaken for 6 h at 100 rpm and ambient temperature and then centrifuged at $6000 \times$ g for 20 min at 4℃. 2 ml of the resultant supernatant was taken for TP, IP and OP analysis. The remaining extracts were freeze-dried again and stored at -20℃ till ^{31}P NMR analysis.

The samples preparation process and detection method by ^{31}P NMR was shown in Chapter 2.2.4.

3.3. Results and discussion

3.3.1. Formation and characterization of nitrifying AGS

The SBRs were operated for 120 days. Granules appeared in the two reactors on day 13 after startup and then grew gradually along with the operation. From day 90 on, the granular size averagely stabilized at 0.76-0.78 mm, although the initial diameter of seed sludge was about 0.17 mm (Table 3-1). This observation is in agreement with the finding by Verawaty et al. (2013) who reported that granules in the reactor equilibrated towards a common critical size of around 0.6-0.8 mm. MLSS and SVI_{30} were determined to be 12-13 g/l and 22 ml/g after 60 days' cultivation. It is worth

noting that the MLVSS/MLSS ratio of granules progressively decreased from 86% to 73% at the end of experiment, probably due to the accumulation of mineral substances, which will be further demonstrated in the following sections. As shown in Figure 3-1a, the yellowish mature granules had irregular shapes, possibly contributed by the square structure of SBRs in this study. SEM observation on day 110 clearly showed the compact and dense structure of the granules, and most of the bacteria were distributed in the outer layer (Figure 3-1b and 1d) with little bacteria in the core of the granules (Figure 3-1b and 1c), which is in agreement with the results from Adav et al. (2008b).

3.3.2. Overall pollutants removal performance

In order to evaluate COD, NH_4-N and PO_4-P removal rates, typical batch experiments were carried out on days 55 and 115, namely the influent NH_4-N concentration was 100 mg/l and 200 mg/l, respectively (Figure 3-2). It was found that COD removal efficiency was about 80% during non-aeration stage, then increased to around 92% after aeration for 30 min and kept this COD removal rate in both cycle tests (data not shown). Figure 3-2a and 2b show that a small amount of NH_4-N was removed during the non-aeration period, probably attributable to heterotrophic assimilation and adsorption by the granules (Bassin et al., 2011). In the subsequent aeration stage, NH_4-N was observed to first convert to NO_2-N and then rapidly to NO_3-N by nitrifying bacteria. Both NH_4-N and NO_2-N were not detectable (99.9% of nitrification) after influent feeding for about 2 h and 3 h when influent NH_4-N concentration was 100 mg/l and 200 mg/l, respectively (Figure 3-2a and 2b). The results indicate that the granules possessed excellent nitrification capacity, about 9 mg NH_4-N/g-VSS·h under the influent COD of 600 mg/l and NH_4-N of 200 mg/l. As shown in Figure 3-2a, on the other hand, PO_4-P was observed to release remarkably during the non-aeration period while P uptake was detected during aeration period

under 100 mg/l of influent NH_4-N concentration, suggesting the presence and activity of PAOs. This phenomenon, however, didn't occur when the influent NH_4-N concentration increased to 200 mg/l (Figure 3-2b), signaling the activity of PAOs might be inhibited by free ammonia. Zheng et al. (2013) claimed that 8.88 mg-N/l of free ammonia initialed the inhibition on PAOs and its toxic threshold concentration for P metabolism would be 17.76 mg-N/l. In this study, the pH of bulk liquor ranged between 7.5 and 8.0, thus free ammonia was maintained at relatively high levels (3.6-11.1 mg-N/l). In addition, only about 1 mg-P/l of P removal (10% of influent P) was achieved through microbial assimilation in these two cycle tests, which is mostly associated with the long SRT (40 days) applied in this study. The above results suggest that the aerobic granules cultivated in this study possessed high nitrification capability while low P removal efficiency.

3.3.3. P fractionation in nitrifying AGS by SMT protocol

Table 3-2 lists the analytical results of P fractions in seed sludge and nitrifying AGS. Seen from Table 3-2 it is clear that the content of each P fraction in seed sludge was much higher than that in nitrifying AGS. This observation may be resulted from the different influent composition and operation strategy between the seed sludge sampled from the wastewater treatment plant and the AGS cultivated in this study. Table 3-2 also shows that the OP content maintained at around 7.5 mg/g-MLSS in AGS during the whole process, suggesting that OP is relatively stable in quantity under the designed operation conditions, which may play an important role in the P recovery from AGS. Although the OP content of seed sludge (15.6 mg/g) was much higher than that of granules (Table 3-2), the percentage of OP to TP for both sludges was quite similar (42.3% in the seed sludge and 39.3-43.3% in the granules sampled between day 30 and day 60, Figure 3-3a). Specifically, it is worth mentioning that the

OP content and percentage in this study were higher than the findings of previous studies (1.4-5.8 mg/g and 9.9-22.3%) (Xie et al., 2011b; Medeiros et al., 2005), which might be brought about by the different drying and storage method used for sludge preparation in this study.

On the other hand, IP was the major P fraction in the seed sludge (57.5% of TP) and nitrifying AGS (61.4-67.7% of TP), in which NAIP amounted to 65.1% and 61.9-70.2% of IP, respectively (Figure 3-3a). In addition, NAIP was about 37.4% and 38.0-47.5% of TP in the seed sludge and nitrifying AGS. Compared with OP and NAIP, AP content was relatively lower and stable, about 20.9% and 18.1-20.1% of TP respectively in the seed sludge and nitrifying AGS.

When the changes in biomass concentration in the reactors were taken into consideration, P mass stored in the sludge could be used for the assessment of P accumulation capability of PAOs. Obviously from Figure 3-3b it can be discerned that before granular maturation (day 30), little accumulation was detected in all the P fractions, although the biomass concentration doubled in the reactors (Table 3-1), possibly due to the absence of PAOs and operation strategy used in this study. Under the same operation conditions including the same influent COD (600 mg/l) and NH_4-N (100 mg/l) concentrations, however, P amount stored in the biomass increased remarkably on day 60 by 80%, 53% and 70% with respect to TP, OP and IP, respectively, although P removal from wastewater was low (Figure 3-2). Nevertheless, this increase trend seemed to retard to some extent when the influent NH_4-N concentration was increased to 200 mg/l, especially for OP. This observation partly coincides with the cycle tests (Figure 3-2). Along with the operation from day 60 to day 120, although P mass in inorganic forms (NAIP and AP) continuously increased,

the OP mass showed much less increment (Figure 3-3b), partially signaling the activity of PAOs was inhibited.

Interestingly, the increase of IP, NAIP and AP in the sludge was found to have close relationship with the amount of metal ions accumulated in the granules, especially Ca and Fe in this work (Table 3-3). The linear correlation coefficient (R^2) was 0.995 between accumulated Fe and NAIP, which was about 0.971 between accumulated Ca and AP content in the sludge. According to the SMT protocol, NAIP is mainly associated with Al, Fe and Mn, while AP is directly related with Ca (Ruban et al., 1999; Pardo et al., 2003). Due to very less amount of Mn and Al in the sludge, it can be inferred that mineral phosphorus is mainly associated with Fe and Ca in NAIP and AP fractions, respectively in this study. NAIP and OP are regarded as potentially releasable and bioavailable P (Ruban et al., 1999; Xie et al., 2011a). In this study, the proportion of NAIP + OP was about 80.9% for both seed sludge and nitrifying AGS (Figure 3-3a). A similar result has been reported by Xie et al. (2011b) who found that NAIP + OP was greater than 85% and 75% of TP in activated sludge samples fed with domestic and industrial wastewaters, respectively. Moreover, a positive correlation ($R^2 = 0.995$) was observed between TP and NAIP + OP in nitrifying AGS during the whole operation. Therefore, it can be concluded that high potentially mobile and bio-available phosphorus could be stored in the nitrifying AGS.

3.3.4. Species of IP in nitrifying AGS by XRD

XRD, an efficient tool for distinguishing crystalline minerals from those of amorphous structure, was used to identify the species of P minerals in the granule samples. As illustrated in Figure 3-4, a number of distinct peaks in the diffractogram reflect the presence of crystalline forms. By comparison with portable document format standard card (2004) using Jade 6.0, most of the stronger peaks coincide with

those of Hydroxyapatite [$Ca_5(PO_4)_3(OH)$] pattern and iron phosphate [$Fe_7(PO_4)_6$] pattern.

Different P minerals have been reported in AGS, such as hydroxyapatite, whitlockite [$Ca_3(PO_4)_2$, $Ca_{18}Mg_2H_2(PO_4)_{14}$] and struvite [$NH_4MgPO_4 \cdot 6H_2O$] in previous studies (Angela et al., 2011; Li et al., 2014; Lin et al., 2012). The result from this study agrees with Angela et al. (2011) who reported that hydroxyapatite was a major phosphate mineral in AGS. In the calcium phosphate family, hydroxyapatite is considered as the most stable and insoluble one. Moreover, the dense structure of granules encouraged the accumulation of P minerals in the core of granules and repressed the solubilization of the crystals. However, no whitlockite or struvite was detected in the granules. As pH and influent composition play an important role on phosphate precipitation due to their influence on the SI of different minerals (Montastruc et al., 2003; Barat et al., 2011; Juang et al., 2010), so in this study SI was also calculated using the Minteq.v3.1 database (PHREEQC software) (Table 3-4). The results show that SI of struvite was negative under the designed conditions in this study, indicating magnesium concentration might be too low to initiate struvite precipitation. The SI of whitlockite was close to zero, implying whitlockite was poorly or very temporarily formed. On the contrary, high level of SI (between 4.78 and 7.66) was obtained for hydroxyapatite, i.e. the most stable phase among the calcium phosphates signaling its oversaturation state in the tested conditions.

In addition, high level of SI for vivianite [$Fe_3(PO_4)_2 \cdot 8H_2O$] was also obtained (Table 3-4). According to the portable document format standard card, the observed XRD peaks do not agree with those of vivianite pattern. However, two major peaks (20.5 and 29.7) of the granular sample could be assigned to another iron phosphate, [$Fe_7(PO_4)_6$] pattern. Under the high DO levels (7-9 mg/l) applied in reactors in this

study, part of Fe^{2+} could be inevitably and easily oxidized to Fe^{3+} and then form the stable crystal of iron phosphate. Moreover, $FePO_4$ crystal can be gradually transformed into $Fe_7(PO_4)_6$ by redox reactions (Gadgil and Kulshreshtha, 1994; Wang et al., 2013) created in the granules. Therefore, it could be confirmed that hydroxyapatite and iron phosphate [$Fe_7(PO_4)_6$] were the major inorganic P in the nitrifying AGS in this study. Still, whether other intermediates present or not remain unknown due to the limitation of XRD for microamount minerals.

3.3.5. Identification of P species in nitrifying AGS by ^{31}P NMR analysis

All NMR-spectra show peaks in the areas for ortho-P (5 to 7 ppm), monoester-P (3 to 5 ppm), diester-P (2 to −3 ppm), pyro-P (−4 to −6 ppm), poly-P (−18 to −21 ppm), and phosphonates (22 to 24 ppm) (Figure 3-5). Monoester-P, diester-P and phosphonates belong to OP, while ortho-P, pyro-P and poly-P are IP.

Although it's difficult to make an exact integration of the peak areas in NMR, the quantification of these compounds with NMR is a suitable method to estimate the relative proportions of P groups (Ahlgren et al., 2005; Zhang et al., 2013). Table 3-5 shows the contents of these P fractions extracted by NaOH + Na_2EDTA method and their relative proportions (% TP) identified by ^{31}P NMR. The average TP content in the NaOH + Na_2EDTA extracts was 17.3 mg-P/g SS with an average extraction rate of approximately 77.6% of TP, which is similar with the result (about 73%) obtained by Turner (2004).

Ortho-P is the dominant P species in the granule extracts, accounting for 74.3% of TP. Ortho-P mainly exists in P form like Fe- and Ca-bound IP and is also the main nutrient for living organisms. Although a low level of 1.9% (of TP) was detected in the granule extracts, pyro-P content in the granules is much higher than those (0.2-0.8%) of lake sediment samples (Zhang et al., 2013). Besides, the presence of

pyro-P signals high microbial activity involved in the biological P cycling in samples (Condron et al., 1985; Ahlgren et al., 2005). On the other hand, only a very small amount of poly-P was extracted, comprising approximately 0.1% of the extractable TP from granules, which is much lower than those (50% of TP) from activated sludge samples with PAOs (Uhlmann et al., 1990). The less amount of poly-P in the granules sampled on day 120 was probably brought about by the inhibition of free ammonia on the activity of PAOs.

Monoester-P is the major form of OP extracted with $NaOH + Na_2EDTA$ from the nitrifying AGS, accounting for about 21.8% of TP. This is in agreement with the previous results from soil and sediment samples. Monoester-P can be directly correlated with microbial, for instance, the glycerol-6- phosphate (nucleotides) found in cell membrane belongs to monoester-P (Ahlgren et al., 2011). In addition, George et al. (2006) reported that the rhizosphere of plant could utilize monoester-P from oxisols after phosphatase hydrolysis. Moreover, algae can assimilate more than 40% of P from monoester-P in a temperate mesotrophic lake (Hernandez et al., 1997). Although only 1.8% of extracted TP in granules, diester-P plays a crucial role in the AGS due to its close relation to deoxyribonucleic acid (DNA-P), lipid (lipids-P) and teichoic acid (Teichoic-P). Thus the quantity of diester-P may be used to indicate the activity and concentration of microorganisms in nitrifying AGS. As Whitton et al. (1991) pointed out that diester-P could be easily absorbed and utilized by plants and blue green algae under certain conditions, the OP fractions including monoester-P and diester-P are believed to play an important role in the potential mobility and bio-availability of P resource from AGS.

3.4. Summary

This study presents the preliminary results of P species and its bio-availability in nitrifying AGS. The following major conclusions could be arrived at:

(1) IP was the primary P fraction in the granules, in which NAIP amounted to 61.9-70.2%. A positive strong correlation (R^2 = 0.971-0.995) was found between the content of IP (NAIP and AP) and that of metal ions (especially Fe and Ca) in the granules. OP content was very stable in quantity during the operation. About 80.9% of TP in nitrifying AGS possesses high potential mobility and bio-availability.

(2) XRD analysis and SI calculation revealed that hydroxyapatite [$Ca_5(PO_4)_3(OH)$] and iron phosphate [$Fe_7(PO_4)_6$] patterns were the main IP species in the nitrifying AGS.

(3) Three OP compounds (monoester-P, diester-P, phosphonates) and three IP compounds (ortho-P, pyro-P and poly-P) were identified by using ^{31}P NMR, respectively. Monoester-P was the dominant P in OP, and less amount of poly-P was detected in the granules, probably attributable to the inhibition of free ammonia on the activity of PAOs.

In this study P removal rate was low due to the inhibition of relatively high free ammonia levels, which could be alleviated with enhanced P removal by adjusting operation strategy. The results from current work imply that nitrifying AGS could be further potentially developed as P resource materials with high amount of bioavailable P.

Table 3-1 Characteristics of granules in the reactors during 120 days' operation

Operation duration (day)	MLSS (g/l)	MLVSS/MLSS (%)	SVI_{30} (ml/g)	Average diameter (mm)
0	3.6	80	81	0.17
30	7.8	86	28	0.38
60	11.5	82	25	0.62
90	12.8	77	22	0.76
120	13.1	73	22	0.78

Table 3-2 Contents of P fractions in sludge by using the SMT extraction protocol

Operation (day)	TP (mg-P/g-MLSS)	OP (mg-P/g-MLSS)	IP (mg-P/g-MLSS)	NAIP (mg-P/g-MLSS)	AP (mg-P/g-MLSS)	NAIP+OP (mg-P/g-MLSS)	Bio-availability (%)
Seed sludge	36.9±0.9	15.6±0.5	21.2±0.7	13.8±0.5	7.7±0.3	29.4±0.8	79.8
30	17.1±0.4	7.4±0.5	10.5±0.3	6.5±0.4	3.1±0.2	13.9±0.7	81.3
60	19.6±0.7	7.7±0.3	12.1±0.6	8.0±0.6	3.7±0.2	15.7±0.7	80.1
90	20.4±0.6	7.3±0.6	13.5±0.5	9.2±0.4	4.1±04.	16.5±0.5	80.9
120	22.3±0.6	7.6±0.4	15.1±0.2	10.6±0.5	4.4±0.3	18.2±0.6	81.6

The data are expressed as mean value ± standard deviation. MLSS, mixed liquor suspended solids; TP, total phosphorus;

OP, organic phosphorus; IP, inorganic phosphorus; NAIP, non-apatite inorganic phosphorus; AP, apatite phosphorus.

Table 3-3 Average metal contents in the nitrifying AGS

Operation duration (day)	Na (mg/g-MLSS)	K (mg/g-MLSS)	Ca (mg/g-MLSS)	Mg (mg/g-MLSS)	Fe (mg/g-MLSS)	Mn (mg/g-MLSS)	Al (mg/g-MLSS)
30	3.7	1.5	4.6	2.7	6.0	0.2	0.1
60	4.1	2.1	6.8	3.7	8.1	0.3	0.2
90	4.3	2.3	8.5	3.5	10.5	0.3	0.3
120	5.5	3.1	10.8	3.9	12.5	0.5	0.3

Table 3-4 Saturation indices (calculated by Visual MINTEQ ver. 3.1) for the supersaturated species under the NH_4-N levels and pH conditions in the bulk liquor in this study

Species	100 mg NH_4-N /l		200 mg NH_4-N /l	
	pH 7.5	pH 8.0	pH 7.5	pH 8.0
$Ca_3(PO_4)_2$ [beta]	-0.6	0.5	-1.1	0.0
Calcite [$CaCO_3$]	-0.4	0.1	-0.3	0.3
Dolomite [$CaMg(CO_3)_2$]	-0.8	0.2	-0.4	0.6
Hydroxyapatite [$Ca_5(PO_4)_3(OH)$]	5.5	7.7	4.8	6.9
Struvite [$MgNH_4PO_4 \cdot 6H_2O$]	-1.8	-1.3	-1.7	-1.2
Vivianite [$Fe_3(PO_4)_2 \cdot 8H_2O$]	6.3	7.4	6.2	7.3

Table 3-5 Contents of different P fractions extracted by NaOH+ Na$_2$EDTA method and their relative proportions

(%TP) identified by ^{31}P NMR in the granules sampled on day 120

TP	IP			OP		
(mg/g-SS)	Ortho-P (%)	Pyro-P (%)	Poly-P (%)	Monoester-P (%)	Diester-P (%)	Phosphonate (%)
17.3	74.3	1.9	0.1	21.8	1.8	0.1
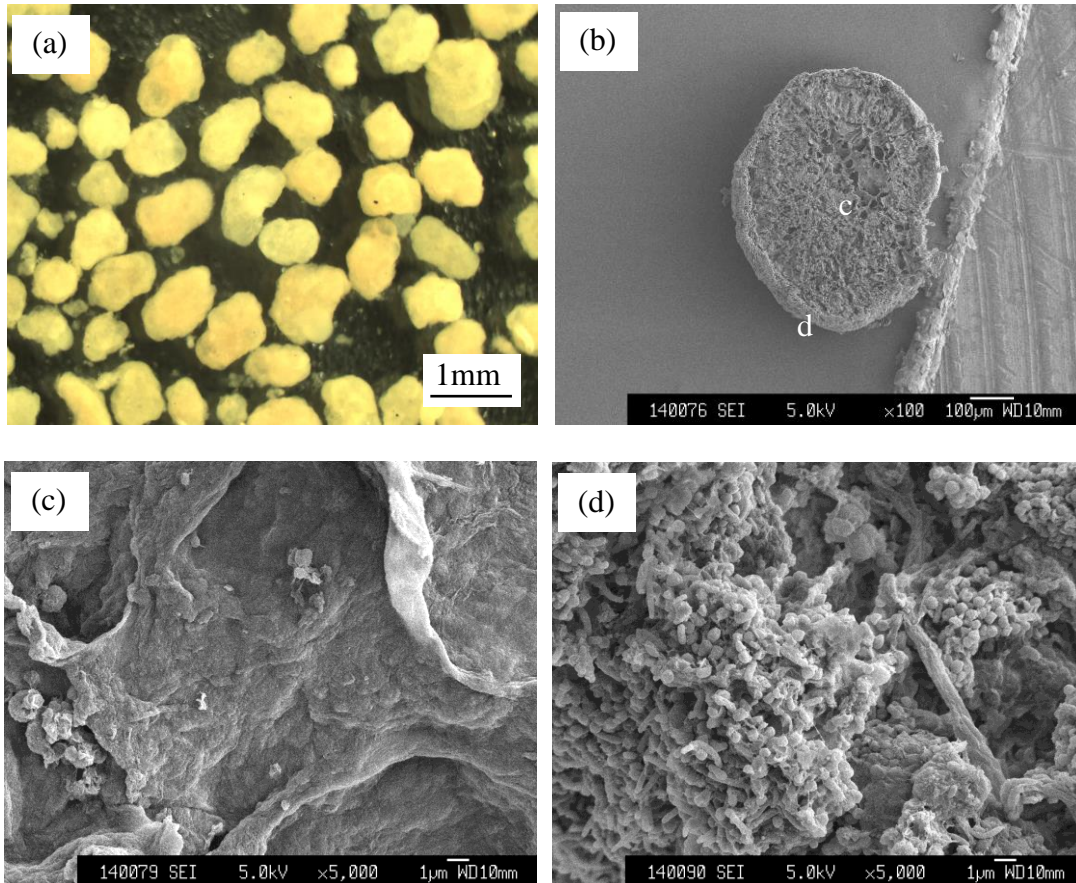
Figure 3-1 Images of the granular sludge on day 110 (Influent NH$_4$-N= 200 mg/l).

Digital image of granules (a), and SEM observation of granules from cross section (b),

core (c) and edge (d) on day 110, respectively.
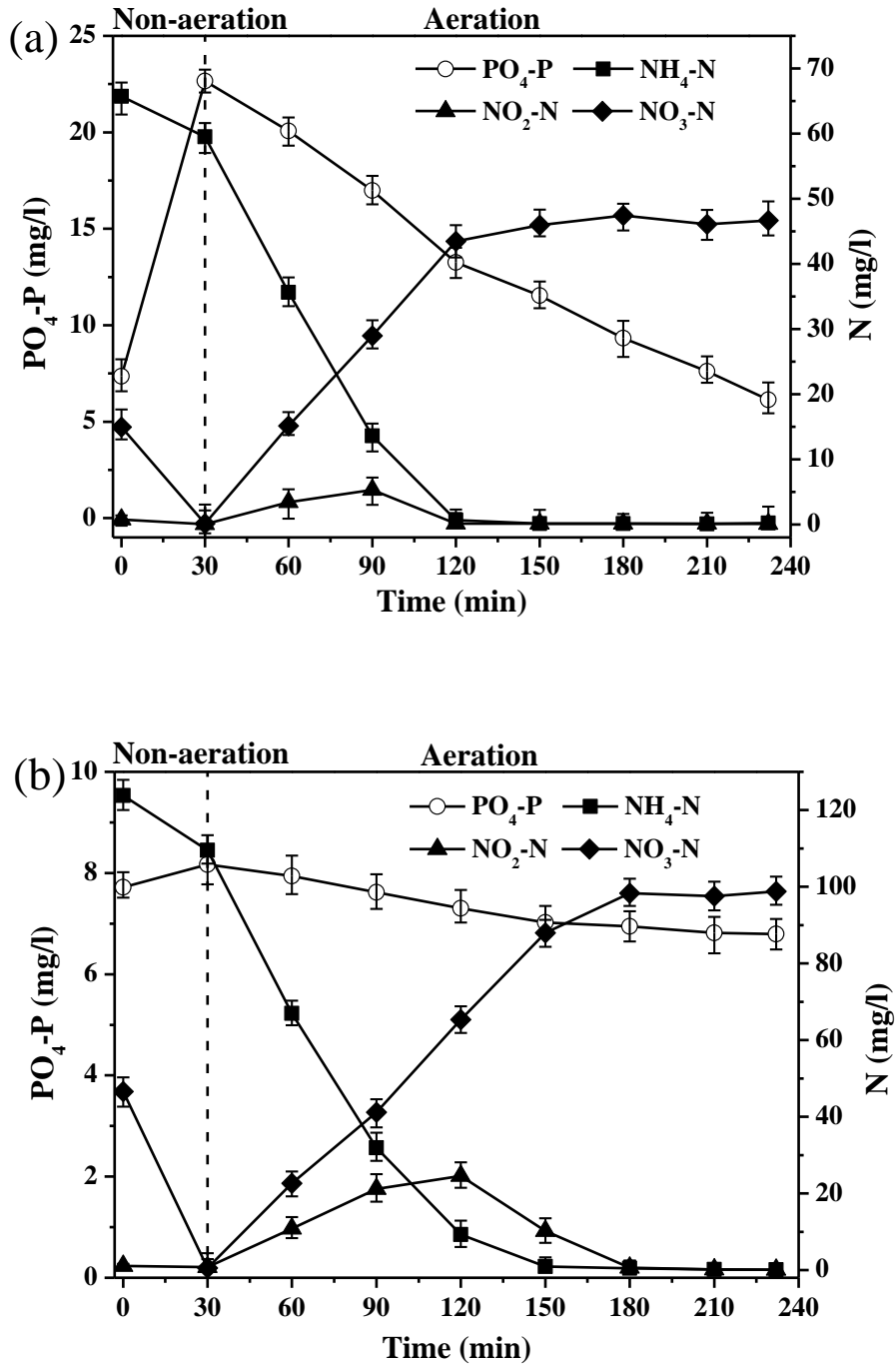
Figure 3-2 Variation of NH_4-N, NO_2-N, NO_3-N and PO_4-P in the bulk liquor during cycle tests under 100 mg/l (a) and 200 mg/l (b) of influent NH_4-N concentration, respectively.
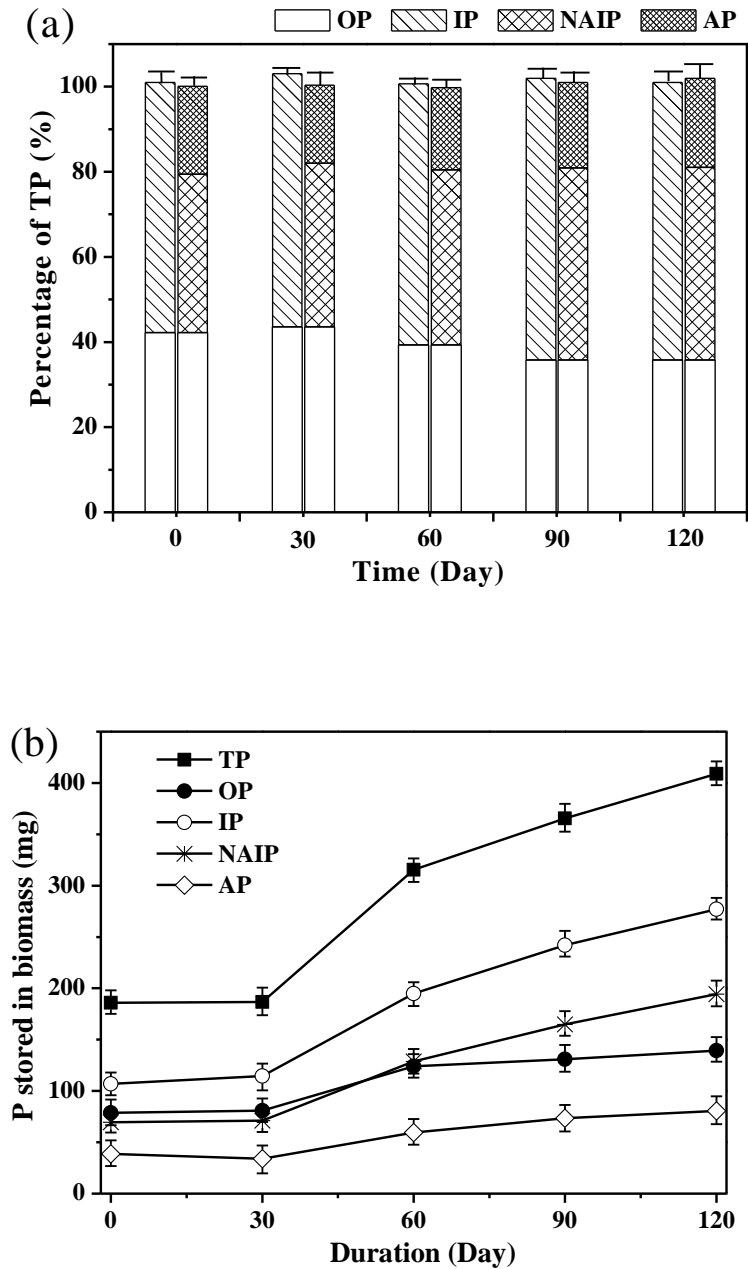
Figure 3-3 Average proportions of phosphorus fractions (%TP) in sludge (a) and changes in P mass stored in biomass in the reactors (b) during 120 days' operation. TP, total phosphorus; OP, organic phosphorus; IP, inorganic phosphorus; NAIP, non-apatite inorganic phosphorus; AP, apatite phosphorus. P stored in biomass is estimated according to the P fraction content and biomass (MLSS) concentration in the reactors.
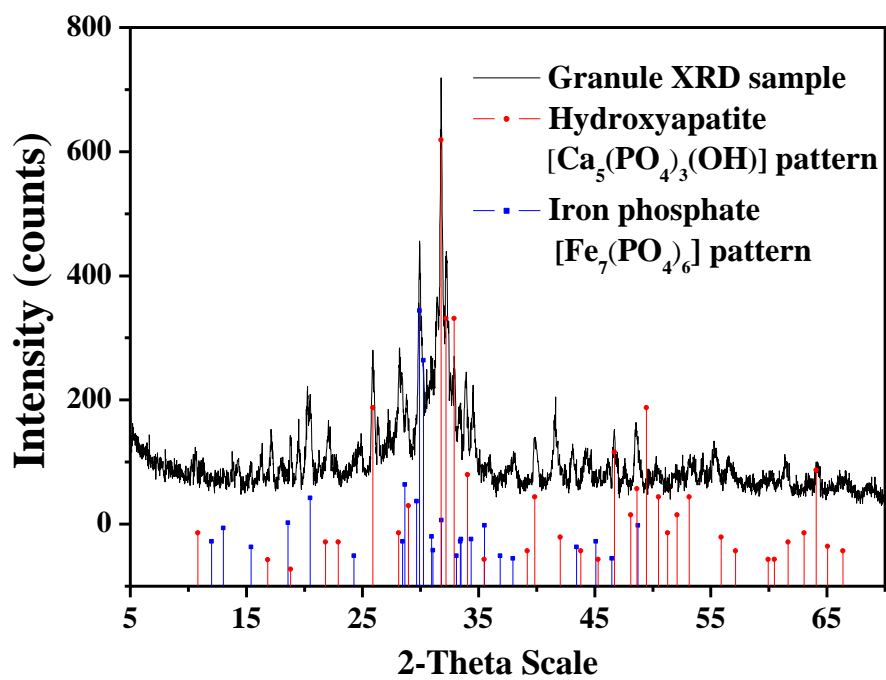
Figure 3-4 XRD diffractogarm of granular sludge compared to standard hydroxyapatite and iron phosphate patterns.
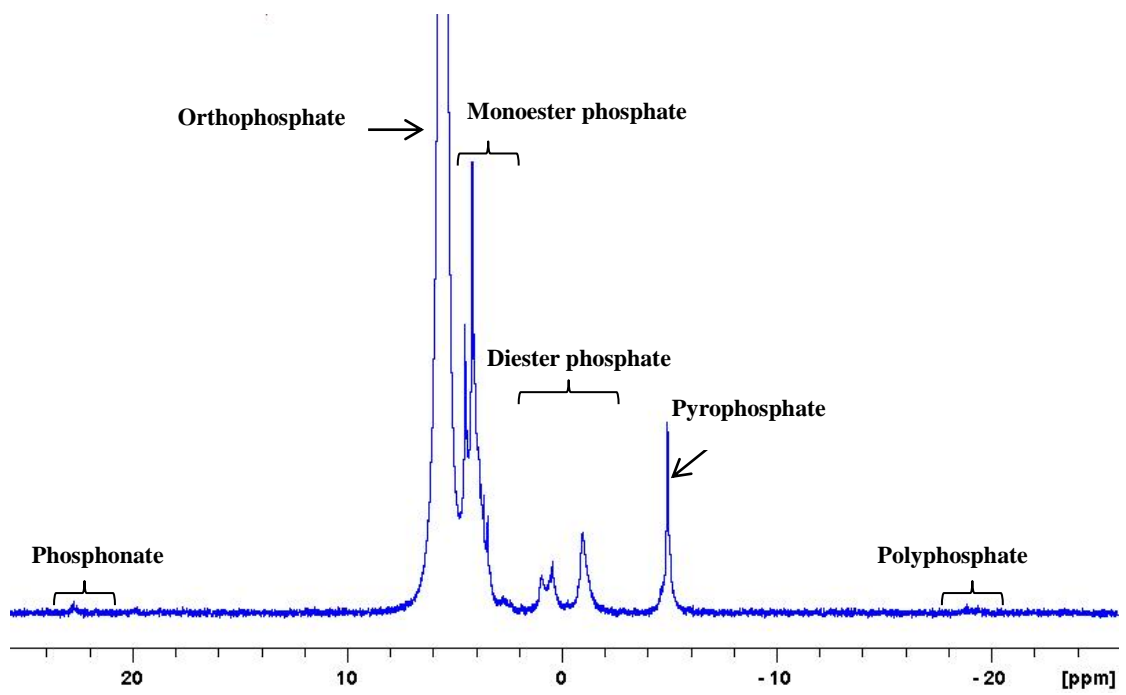
Figure 3-5 Typical ^{31}P-NMR spectra of NaOH+Na$_2$EDTA extracts from the aerobic granules sampled on day 120.

Chapter 4 Distribution and bio-availability of IP and OP species in EBPR-AGS

4.1. Introduction

In an EBPR process, PAOs in AGS can accumulate poly-P through the release of P to bulk liquor in anaerobic phase and then ''luxury uptake'' of P in aerobic phase and P removal is realized by discharging the P-rich AGS (Zhang et al., 2013a). In general, PAOs are mainly regarded to be responsible for P removal in the EBPR process. However, there are some reports that EPS could accumulate plenty of P contributing to P removal as a P reservoir in activated sludge (Zhang et al., 2013a and 2013b; Cloete et al., 2001). Moreover, biologically induced precipitation as the form of hydroxyapatite is estimated to be about 45% of the TP removal in AGS process (Angela et al., 2011). Still, the contribution of cell clusters, EPS, and mineral precipitation to P removal in AGS have not been clearly understood.

On the other hand, it is well known that not all the forms of P exhibit similar mobility and bio-availability which is crucial for the final re-utilization of sludge in agriculture. To date, the mobility and bio-availability of P in the EBPR-AGS is still unknown. In addition, so far, research works on P species and distribution in AGS are mainly focused on mineral P forms (Angela et al., 2011; Li et al., 2014). Nevertheless, P species and the distribution of IP (IP, like ortho-P, pyro-P and poly-P) and IP (OP, like ortho-P monoester-P and diester-P) in AGS, microbial cells and EPS matrix which are closely related with P removal and recovery, has not been documented yet.

This study aimed to investigate the fractionation and distribution of P in the EBPR-AGS and to evaluate the mobility and bio-availability of P accumulated in the

EBPR-AGS. The architectures of the cells, EPS and P distribution in the granules were depicted. IP and OP species in AGS, cells and EPS were further analyzed. Based on the obtained results, P distribution in the granules was conceived to better understand the nature of P in EBPR-AGS, which will help to develop applicable technologies for P removal and recovery from EBPR-AGS through wastewater treatment.

4.2. Materials and methods

4.2.1. Experimental set-up and operation

EBPR-AGS were cultivated in two identical SBRs made of acrylic plastic, 6 cm in diameter with a height of 60 cm, and their effective working volume was 1.4 l. Each reactor was inoculated with 0.5 l of seed sludge sampled from a sedimentation tank of the Shimodate Sewage Treatment Plant, Ibaraki Prefecture, Japan. Compressed air was provided by an air pump (AK-30, KOSHIN, Japan) through air bubble diffusers at the bottom of each reactor with an air flow rate of 1.0 cm/s and the DO varied between 3 - 8 mg/l during aeration. The reactors were operated sequentially in a 4-h cycle at room temperature ($25\pm2℃$): 2 min of influent filling, 58 min of non-aeration period, 156 - 176 min of aeration, 2 - 20 min of settling, and 4 min of effluent discharge. The settling time was gradually decreased from 20 min to 2 min due to the increase in settleability of the sludge. The volumetric exchange ratio was kept at 50％, resulting in a hydraulic retention time of 8 h. After EBPR-AGS appeared, the mixed liquor was withdrawn daily from the reactors in order to keep the SRT averagely around 10 days (varied between 8 and 12 days).

Synthetic wastewater was used in this study, and its composition was as follows: COD 600 mg/l (50% of which was contributed by glucose and sodium acetate, respectively); 20 mg PO_4-P/l (KH_2PO_4); 50 mg NH_4-N/l (NH_4Cl); 10 mg Ca^{2+}/l ($CaCl_2$); 5 mg Mg^{2+}/l ($MgSO_4 \cdot 7H_2O$); 5 mg Fe^{2+}/l ($FeSO_4 \cdot 7H_2O$); and 1ml/l of trace element solution. The pH in the two reactors was adjusted to be within 7.0 - 8.3 with sodium bicarbonate.

4.2.2. P fractionation in EBPR-AGS

In order to avoid the transformation of P species in granules during preparation, the samples taken from the reactors were frozen immediately at -80℃, lyophilized at -50℃ for 48 h and stored at -20℃ until analysis. The SMT Programme extraction protocol was applied to analyze P fractions in the EBPR-AGS and detail has been shown in Figure 2-2.

4.2.3. Extraction and species analysis of P in EBPR-AGS

The samples preparation and extraction method were shown in Figure 2-3. After extraction, neutralization was conducted immediately to minimize P transformation. 2 ml of the resultant supernatant was taken for TP, IP and OP analysis. The remaining extracts were freeze-dried at -50℃ for 48 h and stored at -20℃ till ^{31}P NMR analysis.

4.2.4. Extraction and analysis of P from EPS and cells

Both EDTA and ultrasound approaches are suitable for EPS extraction from sludge and cells because of their low damage to cells structure (Dignac et al., 1998; Sheng et al., 2005; Zhang et al., 2013b). In order to extract EPS and then P from the sludge more efficiently, an EDTA - ultrasound extraction method was applied in this study (Figure 4-1). Similarly, a certain amount of sludge sampled at the end of

aeration cycle was washed twice with 100 mM NaCl solution (4℃) and then centrifuged at 8000 rpm and 4℃ for 5 min. After the supernatant being discarded, the remaining AGS along with 100 ml of 2% EDTA solution was added into a 200 ml beaker and treated at low frequency ultrasound (20 Hz, 120W) in an ice bath for 10 min. Afterwards, the sludge mixture was stirred at 100 rpm and 4℃ for 1 h. Thereafter the suspension was centrifuged at 12, 000 rpm for 20 min, and the supernatant was filtered through 0.22 μm cellulose nitrate membrane filters (Nalgene). The P in the microbial cells was extracted by the same PCA-NaOH method used for AGS as shown in Figure 2-3. Stated, all the extracts were lyophilized at -50℃ for 48 h and then stored at -20℃ till ^{31}P NMR analysis.

4.2.5. CLSM observation of EBPR-AGS

The florescence labeling and CLSM imaging techniques were used to investigate the microbial cells, EPS and poly-P distribution in the EBPR-AGS. All probes were purchased from Molecular Probes (Life Technologies, USA), and the excitation and emission wavelengths for dyes and associated targets are presented in Table 4-1. This study used the microbial cells and EPS staining procedure proposed by Chen et al. (2007). In brief, the SYTO 63 (20 μM, in DMSO, pH 7.2) was first added to the samples for 30 min to stain nucleic acid of all cells. Then the samples were incubated with fluorescein isothiocyanate (FITC) (1 g/l in DMSO) at room temperature for 60 min to stain protein and amino-sugars of the cells and EPS. Subsequently, the Concanavalin A solution (0.2 g/l) was added to the sample and incubated for 30 min for α-D-glucopyranose polysaccharides staining. Finally, the sample was incubated in Calcofluor white to stain β-D-glucopyranose polysaccharides. The excess dye solution was washed with 1×PBS buffer after each staining. The stained granules were sliced

into 100 μm sections after frozen at -20°C, and the sections were then mounted onto a microscopic slide for CLSM (Olympus, FV1000-D) observation.

The fluorescent probe DAPI has been utilized for poly-P observation in activated sludge (Aschar-Sobbi et al., 2008; Hupfer et al., 2008). In this study, the fresh granules sampled from the reactors were sectioned into around 100 μm slices which were then incubated into 10 μM DAPI for 5 min to stain poly-P. The CLSM images were obtained by laser excitation at 405 nm and emission at 550 nm, and the acquisition of images was done in the presence of 10 μM DAPI.

4.2.6. Analytical methods

The extracellular PN in the extracted EPS were determined by Bradford method with bovine serum albumin as standard (Bradford, 1976). PS were measured by using phenol-sulfuric acid method with glucose as standard (Dubois et al., 1956).The other analytical methods have been described respectively in chapter 2 and chapter 3.

4.3. Results and discussion

4.3.1. Characterization of EBPR-AGS

The physical characteristics such as MLSS, MLVSS/MLSS, SVI_{30} and particle size of the sludge were monitored during the 120 days' operation (Table 4-2). Matured AGS were achieved in the SBRs after operation for 90 days with average diameter stabilized at 2.2 - 2.5 mm. MLSS and SVI_{30} were determined to be 5.0 - 5.5 g/l and 33 ml/g after 30 days' cultivation. Being similar with our previous study (Chapter 3.3.1), the MLVSS/MLSS ratio of granules gradually decreased from 83% to 75% at the end of experiments most probably due to the accumulation of mineral substances in the granules. Owing to the stable granules, COD, NH_4-N and PO_4-P removal efficiencies

were averagely 95%, 99% and 98%, respectively in the reactors from day 20 to the end of experiments as shown in Figure 4-2.

Figures 4-3a and 3b-3d present a cross-section image of fresh granules on day 100 and its SEM images. The outer layer and core of the granules were yellowish and transparent, respectively, signaling different compositions in these areas of granules. The SEM observations clearly show that most of the bacteria are distributed in the outer layer while very less bacteria are in the core of the granules. On the contrary, lots of particle-like substances were observed in the core of the granules while very few found in the outer layer of the granules. This observation to a great extent agrees with the statements made by Ren et al. (2008) and Ahlgren et al. (2011) that inorganic minerals are mainly accumulated in the core of granules. Its detail compositions were further explored in the following experiments.

EPS, closely associated with granule formation and stability, were indicated by the sum of PN and PS in this study. The PN and PS contents in the mature granules were maintained around 183.5±13.7 and 56.4±8.1 mg/g-VSS, respectively. PN was the dominant component of EPS in the AGS, with PN/PS ratios always greater than 3. Figures 4-3e to 3h illustrate the fluorescent staining results which were probed at 280 μm from the outer surface of the cross section. Based on the fluorescent intensity images, it can be found that the cells and α-D-glucopyranose PS are accumulated in the outer layer of granules, while β-D-glucopyranose PS are distributed in the whole granules. These findings are to a great extent in agreement with previous studies (Adav et al., 2008b; Chen et al., 2007). Generally, β-D-glucopyranose PS are believed to be the backbone of granules for embedded PN, and α-PS and cells provide support for the structural integrity of granules. It is interesting to find that PN are distributed in the whole granule, which is somewhat similar with the acetate- or phenol-fed

aerobic granules cultivated by Adav et al. (2008b) and Chen et al. (2007). The major difference, i.e., PN are principally in the outer layer in this study while in the core of the granules in the above mentioned works (Adav et al., 2008b; Chen et al., 2007), probably attributable to the different influent characteristics, operation strategies and thus microbial communities which further affect the secretion and distribution of PN in the granules.

4.3.2. P fractionation in EBPR-AGS by SMT protocol

Table 4-3 lists the analytical results of P fractions in the seed sludge and EBPR-AGS. It is clearly to see that the contents of TP, IP, NAIP and AP in the EBPR-AGS were progressively increased with operation, which were much higher than those of the seed sludge. This observation may be contributed by the different influent composition and operation strategy between the seed sludge sampled from the wastewater treatment plant and the aerobic granules cultivated in this study. IP is found to be the major P fraction in the seed sludge (57.3% of TP) and EBPR-AGS (56.7 - 67.6% of TP), in which NAIP amounts to 90.4% and 88.3 - 93.1% of IP, respectively (Figure 4-4). In addition, NAIP is about 51.8% and 53.4 - 60.5% of TP, respectively in the seed sludge and EBPR-AGS. It should be mentioned that poly-P was the main component of NAIP due to the fact that poly-P could be converted into P by using HCl extraction method (Figures 4-5). Compared with NAIP and OP, AP content was relatively lower, about 4.9% and 5.2 - 6.4% of TP respectively in the seed sludge and EBPR-AGS.

On the other hand, Table 4-3 also shows that the OP content keeps at around 17.9 mg/g-MLSS in the EBPR-AGS during the whole process, suggesting that OP is relatively stable in quantity under the designed operation conditions, which may play an important role in P recovery from the EBPR-AGS. Although the OP content in

EBPR-AGS was very stable, the percentage of OP to TP was gradually decreased from 42.8% on day 30 to 31.8% on day 120 due to the significant increase in TP content in the granules. Specifically, it is worth mentioning that the OP content is much higher than the result from chapter 3, about 7.5 mg/g in nitrifying AGS, suggesting the success in P accumulation in the EBPR-AGS by using the operation strategy designed for the EBPR process in this study.

In general, NAIP and OP are considered to be potentially releasable and bio-available P (Xie et al., 2011b; Ruban et al., 1999). In this study, the proportions of NAIP+OP to TP were about 93.7% and 92.4 - 96.4% for seed sludge and mature EBPR-AGS (Figure 4-4). These results are much higher than the previous findings obtained by Xie et al. (2011a), about 40 - 74% in sewage sludge and 80.9% in nitrifying AGS, respectively. Moreover, a positive correlation (R^2= 0.993) has been found between TP and NAIP+OP in the AGS during the whole operation period. Therefore, it can be deduced that high potentially mobile and bio-available P could be stored in the EBPR-AGS under proper operation strategies.

4.3.3. Species of IP in the core of granules by using EDX and XRD

SEM images (Figs. 4-3b and 3d) show that lots of particle-like substances are clustered in the core of granules. To obtain the compositions of these substances, SEM–EDX was used to analyze the mature granules on day 100. As shown in Fig. 4-6, Ca is the dominant metal element with Ca/P atomic ratio of 1.42 in the crystal, indicating calcium phosphate precipitates might be the main substances in the core of EBPR-AGS. Other metal ions such as iron, magnesium and potassium were also contained in the particle-like substances but their amount was much less than Ca. It is also noticeable that plenty of elemental carbon was detected in the crystals, which might be associated with the EPS wrapping the crystals in the core of granules.

XRD analysis was performed on the EBPR-AGS samples for distinguishing crystalline minerals from those of amorphous structure. The diffractogram is presented in Figure 4-7a. As seen from Figure 4-7a, most of the stronger peaks coincide with those of magnesium phosphate $[Mg_2P_2O_7]$, calcium phosphate $[Ca_3(PO_4)_2]$ and hydroxyapatite $[Ca_5(PO_4)_3OH]$ patterns after being compared with the portable document format standard card (2004) using Jade 5.0. The results from this study to a great extent agree with Angela et al. (2011) and Li et al. (2014) who claimed that hydroxyapatite $[Ca_5(PO_4)_3OH]$ and calcium phosphate $[Ca_3(PO_4)_2]$ were the major phosphate minerals in AGS. As stated before, hydroxyapatite is considered as the most stable and insoluble one in the calcium phosphate family. Moreover, the dense structure of granules favors the accumulation of P minerals in the core of granules and may suppress the solubilization of the crystals. SI, a parameter to assess the state of different minerals in the bulk liquor, was also calculated in a typical cycle test (Fig. 4-7b) by using the Minteq.v3.1 database (PHREEQC software). The SI values of calcite, magnesium phosphate and struvite are negative under the designed conditions in this study, i.e. these minerals are not considerably oversaturated to form (Fig. 4-7b). The SI value of calcium phosphate $[Ca_3(PO_4)_2]$ varies from about 0.6 to below 0 after operation for 45 min, implying that calcium phosphate might be formed in the non-aeration phase. High levels of SI (between 1.6 and 7.2) are obtained for hydroxyapatite, signaling its oversaturation state in the tested conditions.

According to the portable document format standard card, the strongest XRD peaks agree with those of magnesium phosphate $[Mg_2P_2O_7]$ pattern (Figure 4-7a). However, magnesium phosphate may be not formed and accumulated in the core of granules due to much lower level of Mg than Ca in the crystals (Figure 4-6) and negative unsaturated index in the bulk liquor (Figure 4-7b). This observation is

probably related to the transformation of poly-P in the PAOs during sample preparation. The general formula of poly-P is $Me_{n+2}P_nO_{3n+1}$, where n indicates the chain length ranging from 1 to 10^6, and Me represents a metal cation like Na, K, and Mg, etc (Bulatovic., 2007). The form of Mg-polyphosphate in the cells of granule may be converted into $Mg_2P_2O_7$ pattern when the sample was calcined in an oven at $500^{\circ}C$ for 2 h before XRD analysis. Restated, the Ca/P atomic ratio is 1.43 for the crystal compounds. As the atomic ratios of $[Ca_5(PO_4)_3(OH)]$ and $[Ca_3(PO_4)_2]$ are 1.67 and 1.5, respectively, other P-precipitates may add some contribution to the lower Ca/P atomic ratio of the crystal compounds in the core of granules. The detailed reason needs further investigation.

From the above results, it can be deduced that $[Ca_5(PO_4)_3(OH)]$ and $[Ca_3(PO_4)_2]$ are the major inorganic P in the core of EBPR-AGS, accounting for about 5.3 - 6.4% of TP removal in this study. Still, whether other intermediates present or not remain unknown due to the limitation of XRD for micro-amount minerals.

4.3.4. Identification and distribution of P species in granules by ^{31}P NMR analysis

Quantification of various P fractions by integrating the peak areas in NMR has been widely used to estimate the relative proportions of P groups. Table 4-4 summarizes the contents of these compounds and their relative proportions (% TP) in AGS, EPS and cells extracts identified by ^{31}P NMR. The average TP content in the PCA + NaOH extracts from AGS was 54.4 mg-P/g-SS with an average extraction rate of approximately 97.1% of TP, indicating the high efficiency of PCA + NaOH procedure for P extraction from sludge. Furthermore, the majority of P was stored in the cells due to the average TP content in the cell extracts was 41.8 mg-P/g-SS, accounting for 73.7% of TP. This observation indicates that the cells in the granules are mainly responsible for P removal in the EBPR-AGS process. In contrast, the

average TP content in EPS extracts was about 13.5 mg-P/g-SS with an average extraction rate of approximately 24.1% of TP. It is worth noting that the AP (crystal form) in the core of granules might be extracted together with EPS from granules by using EDTA-ultrasound extraction method due to the fact that most of the calcium was released into the EPS extracts after the extraction process (Table 4-5). If the AP content was taken out, EPS contained around 9.9 mg-P/g-SS accounting for 17.6% of TP. The result from this study is in consistence with the statements made by Cloete and Oosthuizen (2001) and Zhang et al. (2013b) who found that EPS reserved about 5 - 30% of P in activated sludge, which play a key role in P removal through sludge disposal and can act as a P reservoir.

The percentage of ortho-P in AGS, cells and EPS are 16.6%, 6.9% and 37.5%, respectively, indicating EPS contain the highest ortho-P (3.7 mg-P/g-SS and 6.6% of TP) in EBP-AGS. No matter intracellular or extracellular, ortho-P is the main nutrient for living organisms involving in compound synthesis and energy metabolism. Obviously, it can be seen that poly-P is the major form of P species in AGS, cells, and EPS, accounting for 59.2%, 64.1% and 62.5%, respectively (Table 4-4). The high contents of poly-P in AGS and cells signal the high amount and bioactivity of PAOs in the EBPR-AGS. Compared with poly-P, pyro-P content was relatively lower in both AGS and cells, about 1.4% and 2.1%, respectively, and almost no pyro-P was detected in the extracts of EPS. The presence of pyro-P is directly relating to microbial activity such as ATP hydrolysis in cells and biological P recycling samples.

On the other hand, monoester-P is the dominant OP species in the AGS and cells extracts, occupying approximately 15.1% and 17.6% of TP, respectively. Similar results have been obtained from soil, sediment and nitrifying AGS samples (Ahlgren et al., 2005; Ahlgren et al., 2011). Specifically, almost no OP was detected in EPS,

indicating EDTA+ultrasound approach could effectively extract EPS and P from AGS without cell damage and lysis. According to Ahlgren et al. (2011), monoerster-P like glycerol-6-phosphate is a crucial constituent of membrane in cells. In addition, adenosine monophosphate (i.e. AMP) also belongs to monoerster-P, which plays an important role in energy metabolism. Diester-P content was slightly lower than monoester-P in both AGS and cells, about 7.7% and 9.3% of extracted P from the samples, respectively. Diester-P is closely related to deoxyribonucleic acid (DNA-P), lipid (lipids-P) and teichoic acid (Teichoic-P) in cells. Thus the quantity of diester-P can be used to indicate the activity and concentration of living cells in AGS. Moreover, monoester-P and diester-P could be easily utilized by plants and algae under certain conditions (Whitton et al., 1991; George et al., 2006), which are believed to play an important role in the potential mobility and bio-availability of P resource recovered from the EBPR-AGS.

4.3.5. Possible distribution of P in EBPR-AGS

Figure 4-8 shows the P distribution in the EBP-AGS. According to the P intensity in EDX mapping, most P are distributed in the outer layer of granules (Figure 4-8a), probably attributing to the cells containing the majority of P are located in the outer layer of the granules. CLSM image (Figure 4-8b) also clearly indicates that poly-P are accumulated in the outer layer while little poly-P was detected in the granule interior. This observation implies that not only the poly-P in cells but also the poly-P in EPS are distributed in the outer layer of granules.

According to the above results, P distribution (Figure 4-8c) in the EBPR-AGS is proposed as follows. On one hand, EPS is the backbone of AGS and form a matrix where microbial cells and crystals are clustered in the outer and inner layers, respectively. Cells, EPS and mineral P contributed to around 73.7%, 17.6% and 5.2 -

6.4% of TP accumulated in the EBPR-AGS, respectively. On the other hand, OP (monoester-P and diester-P) and pyro-P directly relating to the microbial metabolism are distributed in the outer layer. Poly-P both in cells and EPS are also accumulated in the outer layer of granules. Ortho-P is probably distributed in the whole granules. In the core of granules, ortho-P mainly associated with Ca forms the Ca-P crystals, while in the outer layer both cells and EPS contain partial ortho-P as detected. More specifically, the ortho-P and poly-P accumulated in the outer layer of EPS play an important role on P removal in the EBPR-AGS process: In the anaerobic phase, PAOs release P (ortho-P or poly-P) into EPS and then into the bulk liquor; under aerobic conditions, PAOs uptake ortho-P from the bulk liquor into microbial cells through the EPS matrix. In addition, due to the high air shear stress in the reactors, there is less possibility of adherence of Ca-P crystals formed in the bulk liquor to the surface or outer layer of granules, which may initial the formation of new granules and accelerate the granulation process. Furthermore, as the granules have porous structure, the Ca-P crystals may be transported into the interior of the granules and tightly entrapped by the EPS. Restated, in the EBPR-AGS Ca-P minerals are accumulated in the core of granules, and all other P species are distributed in the outer layer of granules. Namely, all the bio-available P (92.4 - 96.4% of TP) are located in the outer layer of the granules, signaling its easy P recovery from the EBPR-AGS and further P recycling.

4.4. Summary

EBPR- AGS was obtained in two identical SBRs and its P bio-availability, species and distribution were identified and analyzed in this study. Results showed that 92.4 - 96.4% of TP in the mature EBPR-AGS exhibited high mobility and

bio-availability. The microbial cells, EPS and mineral precipitates respectively contributed 73.7%, 17.6% and 5.2 - 6.4% to the TP of EBPR-AGS. Granular IP was about 56.7 - 67.6% of TP, and OP content stabilized at 17.8 -18.8 mg/g-MLSS in the mature EBPR-AGS. IP species were ortho-P, pyro-P and poly-P among which poly-P occupying 59.2 - 64.1% of TP was the major P species in AGS, cells and EPS. Monoester-P and diester-P were identified as the OP species in the AGS and cells. Furthermore, hydroxyapatite [$Ca_5(PO_4)_3OH$] and calcium phosphate [$Ca_2(PO_4)_3$] were the dominant P minerals accumulated in the core of the granules. Results from CLSM disclosed that the cells along with poly-P were mainly in the outer layer of AGS while EPS were distributed in the whole granules. Based on the above results, the distribution of IP and OP species in AGS has been conceived, which is much meaningful and important for P removal and recovery from the EBPR-AGS through wastewater treatment.

Table 4-1 Excitation and emission wavelengths for dyes and associated targets

Molecular Probe	Excitation (nm)	Emission (nm)	Target
SYTO 63	633	650-700	Total cells
FITC	488	500-540	Protein
Concanavalin A	543	550-600	α-D-glucopyrano polysaccharides
Calcofluor white	400	410-480	β-D-glucopyrano polysaccharides
DAPI	405	550	Polyphosphate

Table 4-2 Characteristics of granules in the two reactors during 120 days' operation (expressed in average)

Operation duration (day)	MLSS (g/l)	MLVSS/MLSS (%)	SVI_{30} (ml/g)	Average diameter (mm)
0	3.2	82	89	0.2
30	4.8	83	37	0.6
60	5.5	80	32	1.7
90	5.1	78	35	2.3
120	5.3	75	34	2.5

Table 4-3 Average content of each P fraction in the sludge by using the SMT extraction protocol

Operation (day)	TP (mg-P/g-MLS)	OP (mg-P/g-MLSS)	IP (mg-P/g-MLSS)	NAIP (mg-P/g-MLSS)	AP (mg-P/g-MLSS)	NAIP+OP (mg-P/g-MLSS)	Bio-availability (%)
Seed sludge	39.8	16.7	22.8	20.6	2.0	37.3	93.7
30	41.6	17.8	23.9	22.3	2.2	40.1	96.4
60	50.1	18.4	32.2	28.4	2.6	46.8	93.4
90	55.6	18.8	36.2	32.6	3.2	51.4	92.4
120	56.1	17.9	37.9	34.0	3.6	51.9	92.5

TP, total phosphorus; OP, organic phosphorus; IP, inorganic phosphorus; NAIP, non-apatite inorganic phosphorus; AP, apatite phosphorus.

Table 4-4 Contents of different P fractions and their relative proportions (%TP) identified by ^{31}P NMR in the granules sampled on day 120

Sample	$TP_{Extract}$	Recovery	IP			OP	
	(mg-P/g-SS)	(%)	Ortho-P (%)	Pyro-P (%)	Poly-P (%)	Monoester-P (%)	Diester-P (%)
AGS	54.4±4.7	97.1±4.3	16.6±6.5	1.4±1.2	59.2±5.7	15.1±4.9	7.7±2.2
Cells	41.8±4.1	73.7±4.8	6.9±5.8	2.1±1.7	64.1±6.2	17.6±6.3	9.3±3.6
EPS extracts	13.5±3.2	24.1±3.6	54.3±5.1	N.D.	45.7±6.8	N.D.	N.D.
(EPS)*	(9.9±2.8)	(17.6±3.1)	(37.5±4.3)	N.D.	(62.5±5.2)	N.D.	N.D.

*The data were obtained after excluding the proportion caused by AP dissolution during the EDTA-ultrasound extraction process.

N.D., not detectable. EPS, extracellular polymeric substances.

Table 4-5 Average metal contents in different extracts and residue before and after EDTA-ultrasound extraction

Sample	Na (mg/g-SS)	K (mg/g-SS)	Mg (mg/g-SS)	Ca (mg/g-SS)
Sludge	5.3	15.6	17.9	12.9
EPS	1.6	4.23	3.7	10.7
Cell	4.1	10.5	13.5	2.3
Residue	0.3	0.4	1.2	0.1
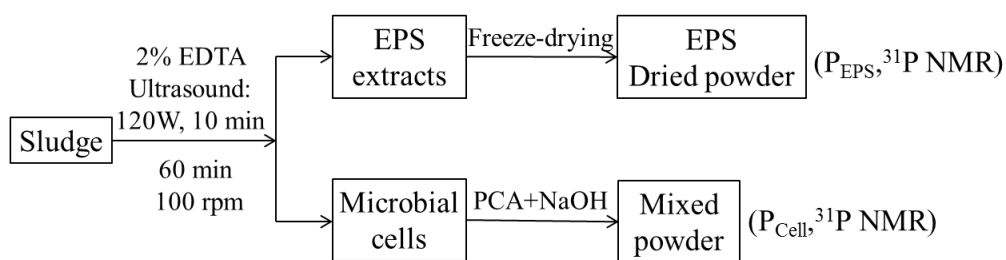
Figure 4-1 Schematic diagrams for the fractionation and characterization of various

forms of P in EPS and cells extracts.
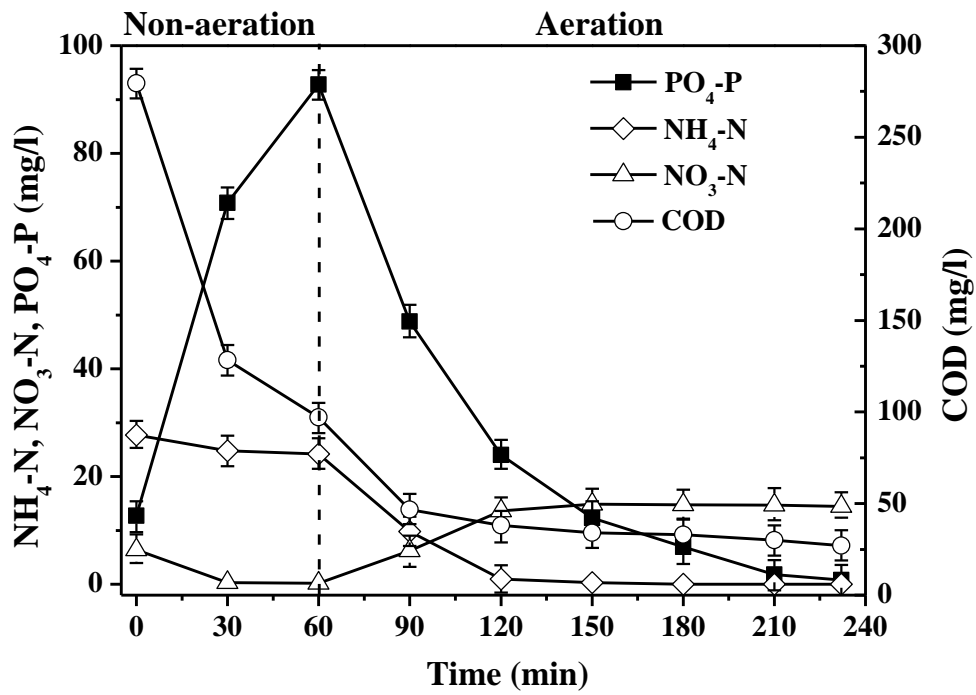
Figure 4-2 Variation of COD, NH$_4$-N, NO$_3$-N and PO$_4$-P in the bulk liquor during

cycle test on day 105.
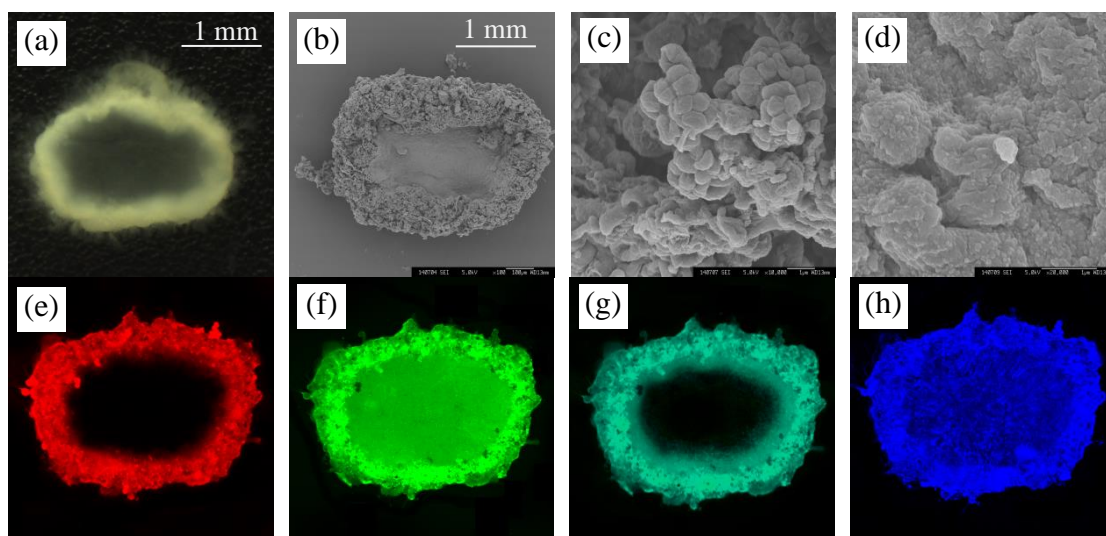
Figure 4-3 Digital image of the cross-section of a fresh granule (a), SEM images from cross section (b), edge (c) and core (d) on day 100, respectively. CLSM images of nucleic acids (SYTO 63, red, e), protein (FITC, green, f), α-D-glucopyranose polysaccharide (Concanavalin A, light blue, g) and β-D-glucopyranose polysaccharide (Calcofluor white, blue, h).
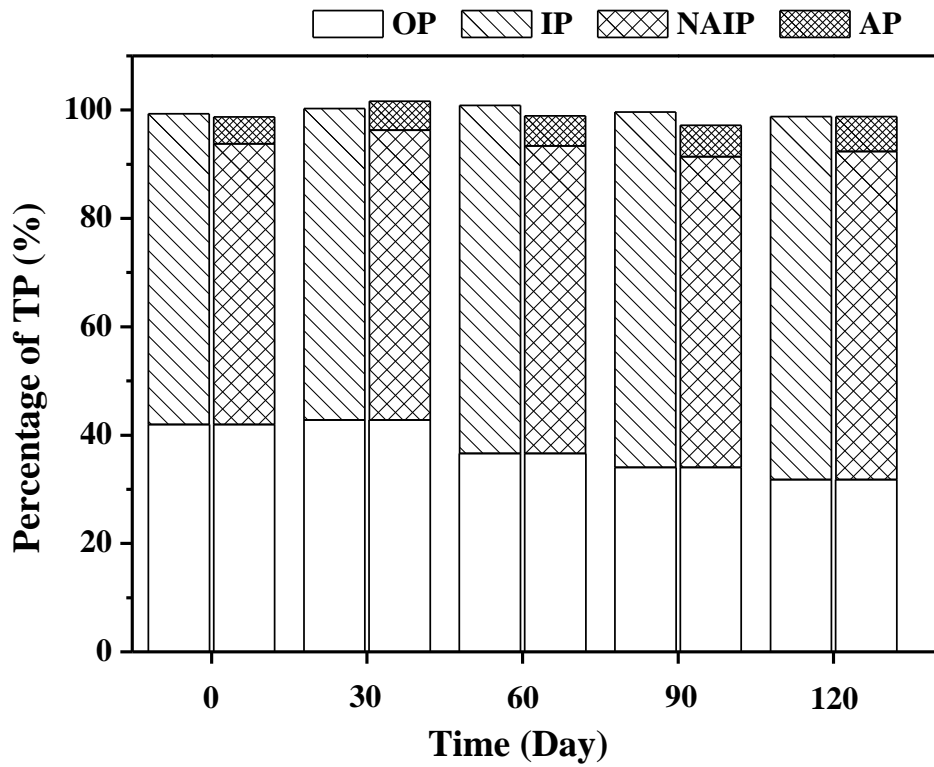
Figure 4-4 Average proportions of P fractions in seed sludge and AGS during the operation. TP, total phosphorus; OP, organic phosphorus; IP, inorganic phosphorus; NAIP, non-apatite inorganic phosphorus; AP, apatite phosphorus.
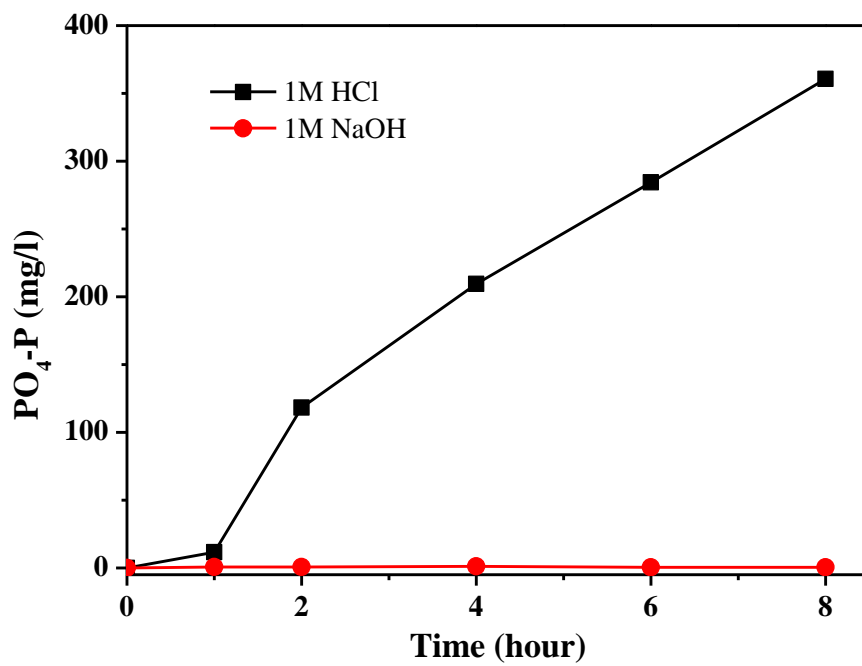
Figure 4-5 Hydrolysis of poly-P (sodium hexametaphosphate) with time in 1 M HCl

and 1M NaOH solution.
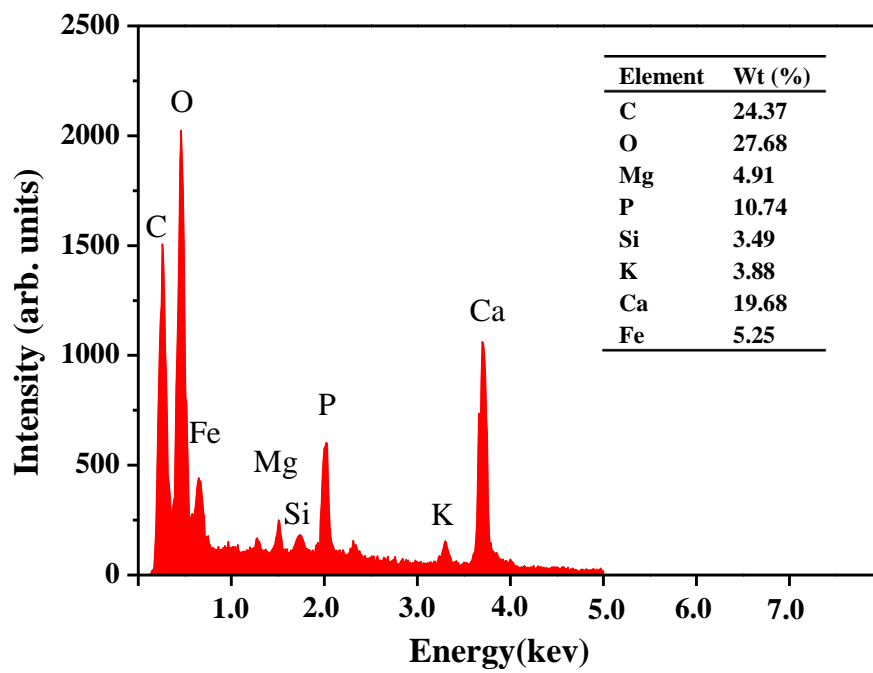
Figure 4-6 EDX spectra of particles in the core of AGS on day 100.
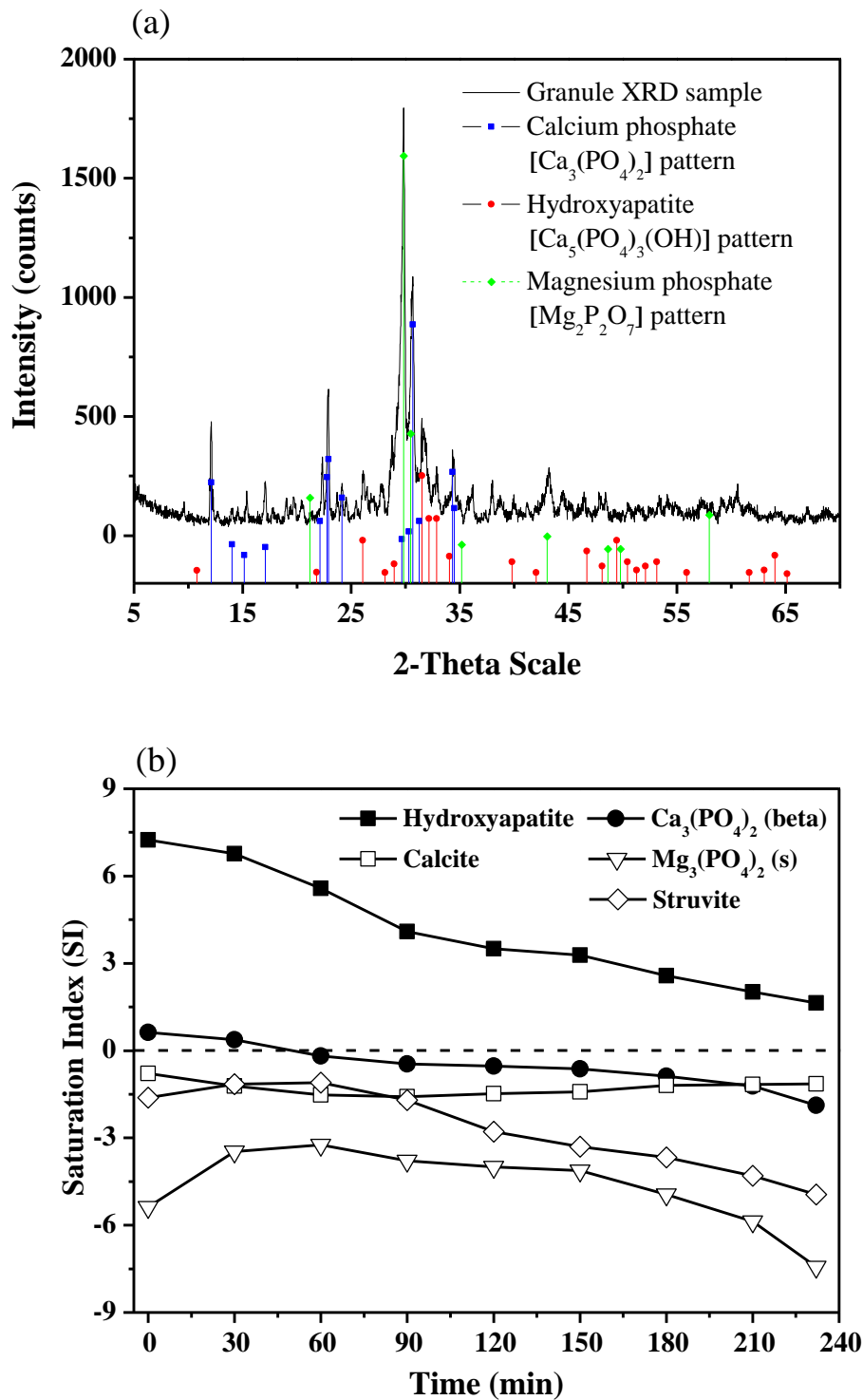
Figure 4-7 XRD diffractogarm of AGS compared to standard calcium phosphate, hydroxyapatite and magnesium phosphate (a), and saturation index for several minerals in the bulk during a typical cycle test on day 110 (b).
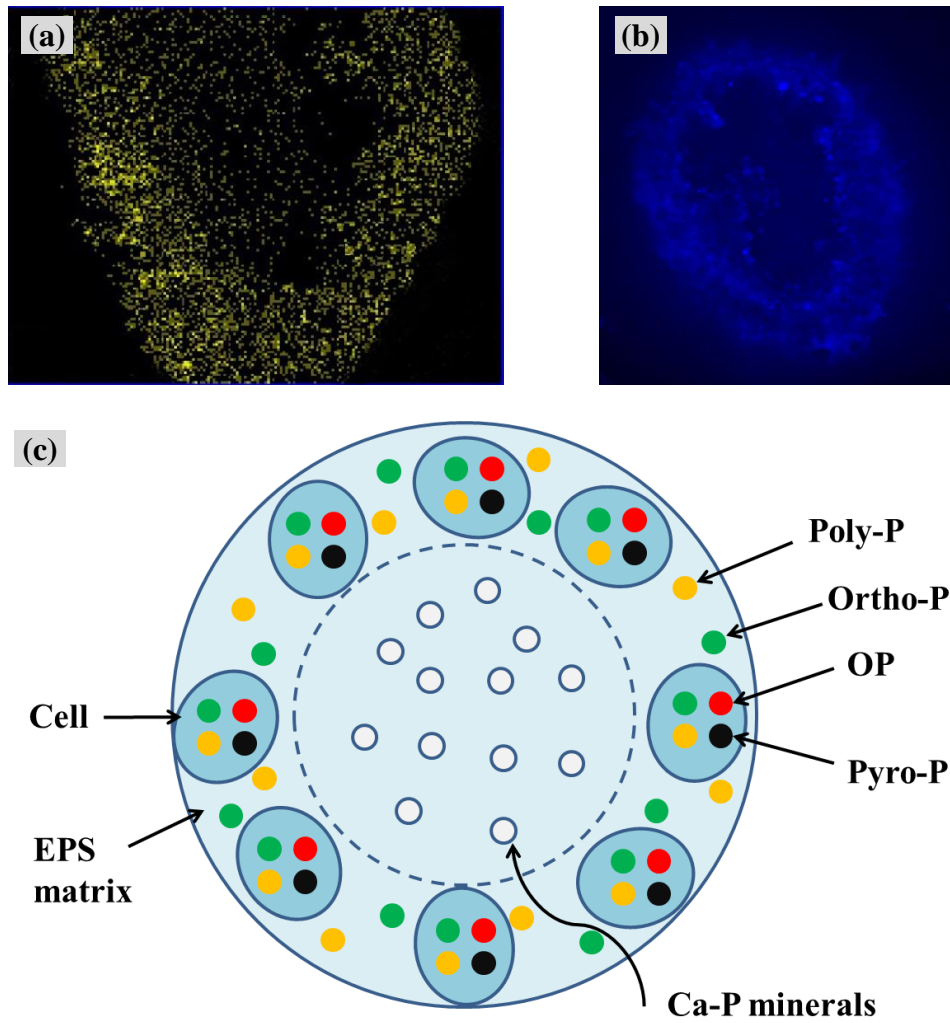
Figure 4-8 EDX mapping of the cross-section of AGS (a), CLSM images of poly-P (DAPI, bright white, b), and schematic diagram of P distribution in AGS (c).

Chapter 5 Conclusions and future research

5.1. Conclusions

In this thesis, the fraction and bio-availability of IP and OP in sewage sludge and AGS were identified and evaluated. The main results are as follows:

(1) About 87.7%, 94.8% 76.2%, 80.9% and 92.4 - 96.4% of TP in primary sludge, secondary sludge, digested sludge, nitrifying AGS and EBPR-AGS, respectively, possesses high potential mobility and bio-availability.

(2) IP was the primary P fraction in the secondary sludge, digested sludge, nitrifying AGS and EBPR-AGS. OP was the dominant P composition in primary sludge.

(3) Monoester-P was the major P species in primary sludge. Monoester-P was also the dominant OP species in all sludges. Ortho-P was the dominant P species in digested sludge and nitrifying AGS. Poly-P was the mainly P species in secondary sludge and EBPR-AGS.

(4) Hydroxyapatite $[Ca_5(PO_4)_3(OH)]$ and iron phosphate $[Fe_7(PO_4)_6)]$ patterns were the main IP species in the nitrifying AGS. Hydroxyapatite $[Ca_5(PO_4)_3OH]$ and calcium phosphate $[Ca_2(PO_4)_3]$ were the dominant P minerals accumulated in the core of EBPR-AGS.

(5) The microbial cells, extracellular polymeric substances (EPS) and mineral precipitates respectively contributed 73.7%, 17.6% and 5.2 - 6.4% to the TP of EBPR-AGS. Poly-P was the major P species in AGS, cells and EPS. Cells along with

poly-P were mainly in the outer layer of AGS while EPS were distributed in the whole granules. Based on the above results, the distribution of IP and OP species in EBPR-AGS has been conceived.

The results of this study will be valuable for P utilization and recovery from sewage sludge and AGS, and provide basic knowledge for the characteristics of P in these sludges and help to develop applicable technologies for P removal and recovery through wastewater treatment.

5.2. Future research

In present study, sewage sludge and AGS showed high P bio-availability. In addition, species and content of IP and OP were different in various sludges. In order to make clear the P removal mechanism by biological method in WWTP and effectively reuse and recover P from sludge, the following aspects should be focused on in the future:

(1) To study the transformation mechanism of P species in different processing units and the mass balance of P in WWTP, such as aeration tank and digestion tank. This will be useful for selecting of various sludges for P recovery.

(2) When sludge is used for agriculture as P fertilizer, it is necessary to explore the influence of some hazardous materials on P accumulation and P reuse, like heavy metals, which will help to develop high-quality and safe P fertilizer from sludge in practice.

(3) In order to recover P from sludge, both P extraction and recovery technology are important. Therefore, finding out cost-effective extraction and recovery methods are necessary.

References

Adav, S.S., Lee, D.-J., Show, K.-Y., Tay, J.-H., 2008a. Aerobic granular sludge: recent advances. Biotechnol. Adv. 26, 411-423.

Adav, S.S., Lee, D.-J., Tay, J.-H., 2008b. Extracellular polymeric substances and structural stability of aerobic granule. Water Res. 42, 1644-1650.

Ahlgren, J., Tranvik, L., Gogoll, A., Waldeback, M., Markides, K., Rydin, E., 2005. Sediment depth attenuation of biogenic phosphorus compounds measured by ^{31}P NMR. Environ. Sci. Technol. 39, 867-872.

Ahlgren, J., Reitzel, K., Brabandere, H.D., Gogoll, A., Rydin, E., 2011. Release of organic P forms from lake sediments. Water Res. 45, 565-572.

APHA,. 1998. Standard Methods for the Examination of Water and Wastewater, 20th ed. American Public Health Association, Washington D.C.

Angela, M., Beatrice, B., Mathieu, S., 2011. Biologically induced phosphorus precipitation in aerobic granular sludge process. Water Res. 45, 3776-3786.

Aschar-Sobbi, R., Abramov, A.Y., Diao, C., Kargacin, M.E., Kargacin, G.J., French, R.J., Pavlov, E., 2008. High sensitivity, quantitative measurements of polyphosphate using a new DAPI-based approach. J. Fluoresc. 18, 859-866.

Bradford, M.M., 1976. A rapid and sensitive method for the quantitation of microgram quantities of protein utilizing the principle of protein-dye binding. Anal. Biochem. 72, 248-254.

Barat, R., Montoya, T., Seco, A., Ferrer, J., 2011. Modelling biological and chemically induced precipitation of calcium phosphate in enhanced biological phosphorus removal systems. Water Res. 45, 3744-3752.

Bassin, J.P., Pronk, M., Kraan, R., Kleerebezem, R., and van Loosdrecht, M.C.M., 2011. Ammonium adsorption in aerobic granular sludge, activated sludge and anammox granules. Water Res. 45, 5257-5265.

Bulatovic, S.M., 2007. Handbook of Flotation Reagents: Chemistry, Theory and Practice. Elsevier B.V., The Netherlands, 1, pp 67.

Chen, M.Y., Lee, D.J., Tay, J.H., 2007. Distribution of extracellular polymeric substances in aerobic granules. Appl. Microbiol. Biotechnol. 73, 1463-1469.

Christen, K., 2007. Closing the phosphorus loop. Environ. Sci. Technol. 41, 2078-2078.

Cloete, T.E., Oosthuizen, D.J., 2001. The role of extracellular exopolymers in the removal of phosphorus from activated sludge. Water Res. 35, 3595-3598.

Condron, L.M., Goh, K.M., Newman, R.H., 1985. Nature and distribution of soil phosphorus as revealed by a sequential extraction method followed by ^{31}P nuclear magnetic resonance analysis. J. Soil Sci. 36, 199-207

Cordell, D., Drangert, J.-O., White, S., 2009. The story of phosphorus: Global food security and food for thought. Global Environ. Chang. 19, 292-305.

Cooper, J., Lombardi, R., Boardman, D., Carliell-Marquet, C., 2011. The future distribution and production of global phosphate rock reserves. Resour. Conserv. Recy. 57, 78-86.

Daumer, M.L., Béline, F., Spérandio, M., Morel, C., 2008. Relevance of a perchloric acid extraction scheme to determine mineral and organic phosphorus in swine slurry. Bioresource Technol. 99, 1319-1324.

Dignac, M.-F., Urbain, V., Rybacki, D., Bruchet, A., Snidaro, D., Scribe, P., 1998. Chemical description of extracellular polymeric substances: implication on activated sludge floc structure. Water Sci. Technol. 38, 45-53.

Dubois, M., Gilles, K.A., Hamilton, J.K., Rebers, P.A., Smith, F., 1956. Colorimetric method for determination of sugars and related substances. Anal. Chem. 28, 350-356.

Franklin, R.J., 2001. Full-scale experiences with anaerobic treatment of industrial wastewater. Water Sci. Technol. 44, 1-6.

Gadgil, M., Kulshreshtha, S., 1994. Study of $FeSO_4$ catalyst. J. Solid State Chem. 111, 357-364.

George, T.S., Turner, B.L., Gregory, P.J., Menun, C.B.J., Richardson, A.E., 2006. Depletionoforganic phosphorus from oxisols in relation to phosphatase activities in the rhizosphere. Eur. J. Soil Sci. 57, 47-57.

He, P., Lü, F., Zhang, H., Shao, L., Lee, D., 2007. Sewage sludge in China: Challenges toward a sustainable future. Water Pract. Technol. 2, 1-8. DOI: 10.2166/wpt.2007. 083

Hernandez, I., Christmas, M., Yelloly, J.M., Whitton, B.A., 1997. Factors affecting surface alkaline phosphatase activity in the brown alga focus spiralis at a North Sea inter tidal site (Tyne sands, Scotland). J. Phycol. 33, 569-575.

Hinedi, Z.R., Chang, A.C. and Lee, R.W.K., 1989. Characterization of phosphorus in sludge extracts using phosphorus-31 nuclear magnetic resonance spectroscopy. J. Environ. Qual. 18, 323-329.

Hupfer, M., Glöss, S., Schmieder, P., Grossart, H.-P., 2008. Methods for detection and quantification of polyphosphate and polyphosphate accumulating microorganisms in aquatic sediments. Internat. Rev. Hydrobiol. 30, 1-30.

IWA Water WIKI, 2015. Global atlas of excreta, wastewater sludge, and biosolids management. http://www.iwawaterwiki.org/xwiki/bin/view/Articles/International

ConferenceonNutrientRecoveryFromWastewaterStreamsVancouver2009?viewer= changes&rev2=21.1(Accessed April 25, 2015)

Jemaat, Z., Suárez-Ojeda, M. E., Pérez, J., Carrera, J., 2014. Partial nitritation and o-cresol removal with aerobic granular biomass in a continuous airlift reactor. Water Res. 48, 354-362.

Juang Y.-C., Adav, S.S., Lee, D.-J., Tay, J.-H., 2010. Stable aerobic granules for continuous-flow reactors: Precipitating calcium and iron salts in granular interiors. Bioresource Technol. 101, 8051-8057.

Karl, D. M., 2000. Aquatic ecology: phosphorus, the staff of life. Nature 406, 31-33.

Kelessidis, A., Stasinakis, A.S., 2012. Comparative study of the methods used for treatment and final disposal of sewage sludge in European countries. Waste Manage. 32, 1186-1195.

Li, M., Zhang, J., Wang G., Yang H., Whelan, M.J., White, S. M., 2013. Organic phosphorus fractionation in wetland soil profiles by chemical extraction and phosphorus-31 nuclear magnetic resonance spectroscopy. Appl. Geochem. 33, 213-221.

Li, Y., Zou J., Zhang, L., Sun, J., 2014. Aerobic granular sludge for simultaneous accumulation of mineral phosphorus and removal of nitrogen via nitrite in wastewater. Bioresource Technol. 154, 178-184.

Lim, S. J., Kim, T.-H., 2014. Applicability and trends of anaerobic granular sludge treatment processes. Biomass and bioenerg. 60, 189-202.

Lin, Y.M., Bassin, J.P, Van Loosdrecht, M.C.M., 2012. The contribution of exopolysaccharides induced struvites accumulation to ammonium adsorption in aerobic granular sludge. Water Res. 46, 986-992.

Liu, Y., Liu, Y.Q., Wang, Z.W., Yang, S.F., Tay, J.H., 2005. Influence of substrate surface loading on the kinetic behaviour of aerobic granules. Appl. Microbiol. Biotechnol. 67, 484-488.

Mahmoud, N., Zeemana, G., Gijzenb, H., Lettinga, G., 2004. Anaerobic sewage treatment in a one-stage UASB reactor and a combined UASB-digester system. Water Res. 38, 2348-2358.

Medeiros, J.J.G., Cid, B.P., Gomez, E.F., 2005. Analytical phosphorus fractionation in sewage sludge and sediment samples. Anal. Bioanal. Chem. 381, 873-878.

Mishima, K., Nakamura, M., 1991. Self-immobilization of aerobic activated sludge-a pilot study of the aerobic upflow sludge blanket process in municipal sewage treatment. Water Sci. Technol. 23, 981-990.

Montastruc, L., Azzaro-P.C., Biscans, B., Cabassud, M., Domenech, S., 2003. A thermochemical approach for calcium phosphate precipitation modeling in a pellet reactor. Chem. Eng. J. 94, 41-50.

Mosquera-Corral, A., de Kreuk, M.K., Heijnen, J.J., van Loosdrecht, M.C.M., 2005. Effects of oxygen concentration on N-removal in an aerobic granular sludge reactor. Water Res. 39, 2676-2686.

Nereda, 2015. Nereda WWTP's on 4 continents. http://www.royalhaskoningdhv.com/en-gb/nereda (Accessed April 18, 2015).

Pardo, P., Lopez-S, F.F., Rauret, G., 2003. Relationships between phosphorus fractionation and major components in sediments using the SMT harmonised extraction procedure. Anal. Bioanal. Chem. 376, 248-254.

Pavšič, P., Mladenovič, A., Mauko, A., Kramar, S., Dolenec, M., Vončina, E., Pavšič Vrtač, K., Bukovec, P., 2014. Sewage sludge/biomass ash based products for sustainable construction. J. Clean. Prod. 67, 117-124.

Qin, L., Tay, J.-H., Liu, Y., 2004. Selection pressure is a driving force of aerobic granulation in sequencing batch reactors. Process Biochem. 39, 579-584.

Ren, T.-T., Liu, L., Sheng, G.-P., Liu, X.-W., Yu, H.-Q., Zhang, M.-C., Zhu, J.-R., 2008. Calcium spatial distribution in aerobic granules and its effects on granule structure, strength and bioactivity. Water Res. 42, 3343-3352.

Ruban, V., Lopez-Sanchez, J.F., Pardo, P., Rauret, G., Muntau, H., Quevauviller, P., 1999. Selection and evaluation of sequential extraction procedures for the determination of phosphorus forms in lake sediment. J. Environ. Monitor. 1, 51-56.

Sheng, G.-P., Yu, H.Q., Yu, Z., 2005. Extraction of the extracellular polymeric substances from a photosynthetic bacterium Rhodopseudomonas acidophila. Appl. Microbiol. Biot. 67, 125-130.

Singh, R.P., Agrawal, M., 2008. Potential benefits and risks of land application of sewage sludge. Waste Manage. 28, 347-358.

Turner, B.L., Mahieu, N., Condron, L.M., 2003. Phosphorus-31 nuclear magnetic resonance spectral assignments of phosphorus compounds in soil NaOH–EDTA extracts. Soil Sci. Soc. Am. J. 67, 497-510.

Turner, B.L., 2004. Optimizing phosphorus characterization in animal manures by solution phosphorus- 31 nuclear magnetic resonance spectroscopy. J. Environ. Qual. 33, 757-766.

Uhlmann, D., Röske, I., Hupfer, M., Ohms, G., 1990. A simple method to distinguish between polyphosphate and other phosphate fractions of activated sludge. Water Res. 24, 1355-1360.

USGS, 2014. Phosphate Rock in Mineral Commodity Summaries. U.S. Geological Survey, Washington D.C.

Van Vuuren, D.P., Bouwmana, A.F., Beusen, A.H.W., 2010. Phosphorus demand for the 1970–2100 period: A scenario analysis of resource depletion. Global Environ. Chang. 20, 428-439.

Verawaty, M., Tait, S., Pijuan, M., Yuan, Z., Bond, P.L., 2013. Breakage and growth towards a stable aerobic granule size during the treatment of wastewater. Water Res. 47, 5338-5349.

Vestergren, J., Vincent, A.G., Jansson, M., Persson, P., Ilstedt, U., Gröbner, G., Giesler, R., Schleucher, J., 2012. High-resolution characterization of organic phosphorus in soil extracts using 2D ^{1}H$-^{31}$P NMR correlation spectroscopy. Environ. Sci. Technol. 46, 3950-3956.

Wang, M., 1997. Land application of sewage sludge in China. Sci. Total Environ. 197, 149-160.

Wang, R., Lin, R., Ding, Y., Liu, J., Wang, J., Zhang, T., 2013. Structure and phase analysis of one-pot hydrothermally synthesized FePO$_4$-SBA-15 as an extremely stable catalyst for harsh oxy-bromination of methane. Appl. Catal. A-Gen. 453, 235-243.

Wang, X.-H., Diao, M.-H., Yang, Y., Shi, Y.-J., Gao, M.-M., Wang, S.-G., 2012. Enhanced aerobic nitrifying granulation by static magnetic field. Bioresource. Technol. 110, 105-110.

Whitton, B.A., Grainger, S.L.J., Hawley, G.R., Simon, J.W., 1991. Cell bound and extra cellular phosphatase activities of cyanobacterial isolates. Microbial Ecol. 21, 85-98.

Xie, C., Tang, J., Zhao, J., Wu, D., Xu, X., 2011a. Comparison of phosphorus fractions and alkaline phosphatase activity in sludge, soils, and sediments. J. Soil. Sediment. 11, 1432-1439.

Xie, C., Zhao, J., Tang, J., Xu, J., Lin, X., Xu X., 2011b. The phosphorus fractions and alkaline phosphatase activities in sludge. Bioresource Technol. 102, 2455-2461.

Xu, H., Zhang, H., Shao, L., He, P., 2012. Fraction distributions of phosphorus in sewage sludge and sludge ash. Waste Biomass Valoriz. 3, 355-361.

Yilmaz, G., Lemaire, R., Keller, J., Yuan, Z.G., 2008. Simultaneous nitrification, denitrification, and phosphorus removal from nutrient-rich industrial wastewater using granular sludge. Biotechnol. Bioeng. 100, 529-541.

Young, J.C., McCarty, P.L., 1969. The anaerobic filter for wastewater treatment. J. Water Pollut. Control Fed. 41, 160-73.

Zhang, H.-L., Fang, W., Wang, Y.-P., Sheng, G.-P., Zeng, R.J., Li, W.-W., Yu, H.-Q., 2013a. Phosphorus removal in an enhanced biological phosphorus removal process: roles of extracellular polymeric substances. Environ. Sci. Technol. 47, 11482-11489.

Zhang, H.-L., Fang, W., Wang, Y.-P., Sheng, G.-P., Xia, C.-W., Zeng, R.J., Yu, H.-Q., 2013b. Species of phosphorus in the extracellular polymeric substances of EBPR sludge. Bioresource Technol. 142, 714-718

Zhang, L., Wang, S., Jiao, L., Ni, Z., Xia, H., Liao, J., Zhu, C., 2013. Characteristics of phosphorus species identified by ^{31}P NMR in different trophic lake sediments from the Eastern Plain, China. Ecol. Eng. 60, 336-343.

Zheng, X., Sun, P., Lou J., Cai, J., Song, Y., Yu, S., Lu, X., 2013. Inhibition of free ammonia to the granule-based enhanced biological phosphorus removal system and the recoverability. Bioresource Technol. 148, 343-351.

Acknowledgements

How time flies. Three years will soon pass, and my overseas study will be over after these 3 wonderful years stay here. Today, I think it's time to say thank you to all the people who gave me help and guidance all the time not only to my study and research, but also to my life.

First of all I would like to say thank you from the bottom of my heart to my supervisors, dear Professor Zhengya Zhang, Professor Zhongfang Lei and Professor Chuanping Feng, for giving me the opportunity to study for a doctoral degree in Japan, and their careful guidance and kindness always make me feel optimistic to face all the problems I met in my research and life.

Secondly, I want to say thanks to the China Scholarship Council (CSC) for the precious scholarship. Because of this scholarship, I could continue my study and research with energy and enough time.

Thirdly, special thanks should go to my thesis committee members, Professor Zhenya Zhang, Zhongfang Lei, Motoo Utsumi and Keiko Yamaji for their patient reading and listening, valuable suggestions and comments. All the instructors provided great help for the improvement of my dissertation and future study.

Fourthly, I want to say thank you to all the members of our laboratory. Thanks for your help in the colorful years when we study and work together. Whenever, I have a question, we can communicate together.

Finally, I would like to express my gratitude to my family. They are always standing by me to give support and make me feel strong.

Publications

[1] **<u>Wenli Huang</u>**, Wei Cai, He Huang, Zhongfang Lei, Zhenya Zhang, Joo Hwa Tay, Duu-Jong Lee, 2015. Identification of inorganic and organic species of phosphorus and its bio-availability in nitrifying aerobic granular sludge. **Water Research**, 68, 423-431.

[2] **<u>Wenli Huang</u>**, Wenlong Wang, Wansheng Shi, Zhongfang Lei, Zhenya Zhang, Rongzhi Chen, 2014. Use low direct current electric field to augment nitrification and structural stability of aerobic granular sludge when treating low COD/NH_4-N wastewater. **Bioresource Technology**, 171, 139-144.

[3] **<u>Wenli Huang</u>**, Bing Li, Chao Zhang, Zhenya Zhang, Zhongfang Lei, Baowang Lu, Beibei Zhou, 2015. Effect of algae growth on aerobic granulation and nutrients removal from synthetic wastewater by using sequencing batch reactors. **Bioresource Technology**, 179, 187-192.

[4] Bing Li, **<u>Wenli Huang</u>** (co-first author), Chao Zhang, Sisi Feng, Zhenya Zhang, Zhongfang Lei, Norio Sugiura, 2015. Effect of TiO_2 nanoparticles on aerobic granulation of algal–bacterial symbiosis system and nutrients removal from synthetic wastewater. **Bioresource Technology**, 187, 214-220.

[5] Wansheng Shi, Chuanping Feng, **<u>Wenli Huang</u>**, Zhongfang Lei, Zhenya Zhang, 2014. Study on interaction between phosphorus and cadmium in sewage sludge during hydrothermal treatment by adding hydroxyapatite. **Bioresource Technology**, 159, 176-181.